

Spatio-temporal Geostatistical Modeling of Hydrogeochemical Parameters in the San Diego Aquifer, Venezuela

¹Dr. Adriana Márquez Romance, ²Dr. Edilberto Guevara Pérez, ³Dr. Demetrio Rey Lago
^{1, 2, 3}Professor,

^{1, 2}Center of Hydrological and Environmental Research, University of Carabobo, Venezuela

³Institute of Mathematics and Compute Applied, University of Carabobo, Venezuela

Email: ¹ammarquez@uc.edu.ve, ²eguevara@uc.edu.ve, ³drey@uc.edu.ve

Abstract

The study is developed a spatio-temporal geostatistical modeling of hydrogeochemical parameters in the San Diego aquifer, Carabobo State, Venezuela during the period 2015-2017. The main water compositions corresponding to the water classes are: 1) Bicarbonate of Calcium and/or Magnesium Ca-Mg-HCO_3 (North and Central regions, 95.16 km², 81.25%) 2) Bicarbonate of Sodium Na-HCO_3 (Central and South regions, 19.32 km², 16.5%), 3) Sulfate or Chloride of Calcium and/or Magnesium Ca-Mg-SO_4 and Ca-Mg-Cl (South region, 0.96 km², 0.82%), 4) Sulfate and/or Chloride of Sodium Na-SO_4 and Na-Cl (South region, 1.68 km², 1.43%). The modeling of the whole hydrogeochemical parameters is represented by J-Bessel function.

Keywords: Hydrogeochemical, Geostatistical Modeling, Spatio-Temporal Distribution.

INTRODUCTION

The San Diego aquifer is an important water source, mainly for domestic uses. The population in San Diego Municipality changes from 59247 in 2001 to 93257 persons in 2011, being increased in 57.4 % in ten years (INE, 2001, 2011). This population increase has created a high pressure on the exploitation of the groundwater resources reaching to 107 pumping wells, having information on hydrogeochemical parameters only of 58 pumping wells by the regulatory institutions in the study zone. In that sense, the Center of Hydrological and Environmental Research of the University of Carabobo has developed and advised scientific studies, measuring hydrogeochemical parameters with a frequency coinciding with climatic season of each year from 2015 to the present in the San Diego aquifer, working in cooperation with the main regulatory entities such as Ministry of Environment and the hydrological company, in order to contributing to the preserve the water quantity and quality available to domestic and industrial uses of the San Diego

aquifer. This investigation has as objectives: a) the analysis of geophysical parameters, land cover and land uses and lithological profiles to classify the type of aquifer, b) to calibrate geostatistical models for representing the spatio-temporal variation of the hydrogeochemical parameters, and c) to generate the maps of spatio-temporal distribution of the hydrogeochemical parameters.

STUDY AREA

The study area is the San Diego aquifer, located in the north region of Venezuela (Figure 1). The aquifer limits in geographic coordinates are the following: latitude: N 10°22'00", N 10°09'00", longitude: W67°52'00", W68°00'00". The San Diego aquifer is belonging to the Carabobo State. The north region is part of the mountain zone of the "Cordillera de la Costa", which is in front of the Caribbean sea (Figure 1). The south region of the San Diego aquifer shares its limits with the Valencia Lake. This aquifer might be interchanging its groundwater with the water body of Valencia Lake according to

the climatic season of the year. The area covered by the San Diego aquifer is 117 km². The perimeter is 95 km. The terrain elevations of the San Diego aquifer are: minimum of 1416 masl, mean: 655 masl and maximum: 1964 masl. The terrain elevation covers area as follows (Figure 1): 1) from 416 to 581 masl (73 km², 63%), 2) from 582 to 891 masl (22 km², 19%), 3) from 892 to 1284 masl (13 km², 11%) and 4) from 1265 to 1264 masl (9 km², 7%). The San Diego aquifer supplies water from 58 pumping wells, which have an use of type: domestic (42, 73%), industrial (16, 27%). The domestic use is based on the water consumption by a population of 93257 persons, being 4.15% of total population of Carabobo State, which is 2.245.744 (INE, 2011).

MATERIALS AND METHODS

The study is developed following the three stages as it is shown in Figure 2, where it can be observed the workflow for spatio-temporal geostatistical modeling of hydrogeochemical parameters in the San Diego aquifer, Carabobo State, Venezuela; which includes: 1) Collection of information as: a) Meteorological, b) Lithological profiles, c) pumping flow, d) water dynamic levels, e) Landsat Satellite Images and f) Digital Elevation Model. 2) Processing of information, including: a) Calibration of geostatistical models, b) validation of geostatistical models, c) calibration of forecast model, and d) application of forecast model. 3) Generation of Results, including: maps of the hydrogeochemical parameters showing spatio-temporal distribution of following parameters: Precipitation, Evapotranspiration, Pumping Flow, Infiltration, Volume Stored, Physico-chemical Parameters (PCP), Hydraulic Parameters, Mass Flow of PCP.

The database used in this study has been provided by four information sources, which are 1) Ministry of the Environment,

2) National Institute of Meteorology and Hydrology belonging to Ministry of the Environment, 3) the Hydrological Company “Hidrologica Del Centro C.A.”, 4) Center of Hydrological and environmental Research. The information has been gotten as it is described in the following four aspects : 1) Meteorological information corresponding to the period between 2015 and 2017, which are measured by the telemetric network of 31 climate monitoring stations close to San Diego aquifer managed by the National Institute of Meteorology and Hydrology belonging to Ministry of the Environment (Table 1). In Table 1 can be observed the details identifying the meteorological stations as: projected coordinates under the following projection parameters: a) Projection: Universal Transverse Mercator (UTM), b) Datum: World Geodetic System 1984 (WGS84), c) UTM Zone: 19 N. The information is available at no cost in the following web page: http://estaciones.inameh.gob.ve/estaciones/estaciones_home.php.___2) Lithological profiles are 28 points located in the north, central and south regions of the San Diego aquifer provided by the Ministry of the Environment (Figure 3, Table 2). 3) The database of water levels, physico-chemical parameters and pumping flow is provided by three sources: a) the Hydrological Company “Hidrologica del Centro C.A.”, consisting of 200 pumping wells in the Carabobo State, b) Ministry of the Environment, consisting of 1201 pumping wells in the Carabobo State and c) Center of Hydrological and Environmental Research of University of Carabobo based on 24 pumping wells into the San Diego aquifer. 4) The information of Landsat Satellite images and ASTER digital elevation model is gotten from the web page identified as earthexplorer belonging to the U.S. Geological Survey (USGS) in the following link: <https://earthexplorer.usgs.gov/>.

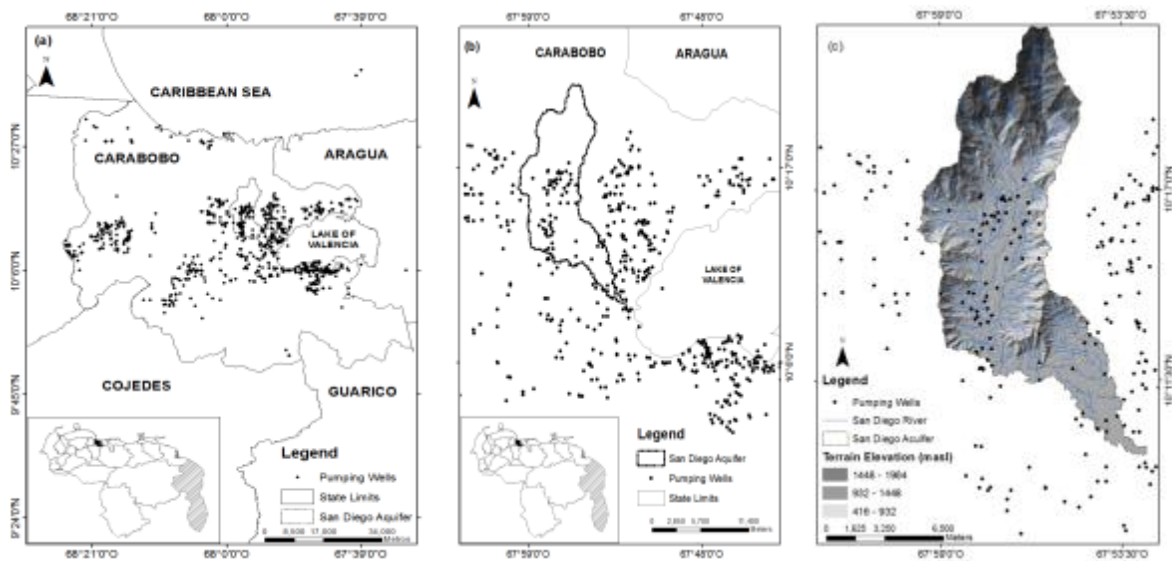


Fig: 1. Location of the study area: a) Relative position of the San Diego aquifer regarding to the Carabobo State in Venezuela, showing the spatial distribution of the 925 pumping wells founded into the Carabobo State; whose monitoring variables are used to predict the hydrogeological parameters from the San Diego aquifer; b) relative position of the San Diego aquifer and pumping wells with respect to the Lake of Valencia; c) Terrain Elevation (masl) and stream network of the San Diego river superimposing the pumping wells. The terrain elevation varies between 416 and 1448masl.

Modeling of Statistical Spatial Prediction

It will be applied models of statistical spatial prediction (SSPM) for estimating of the hydrogeochemical parameters. A spatial prediction model estimates the values of the target variable (z) at some new location s_0 ; being a set of observations of a target variable z denoted as $z(s_1), z(s_2), \dots, z(s_n)$, where $s_i = (x_i, y_i)$ is a location and x_i and y_i are the coordinates (primary locations) in geographical space and n is the number of observations. The geographical domain of interest (area, land surface, object) can be denoted as A . It defines inputs, outputs and the computational procedure to derive outputs based on the given inputs (Hengl, 2007):

$$\hat{z}(s_0) = E\{Z/z(s_i), q_k(s_0), \gamma(h), s \in A\}$$

Where $z(s_i)$ is the input point dataset, $q_k(s_0)$ is the list of deterministic predictors and $\gamma(h)$ is the covariance model defining the spatial autocorrelation structure. The type

of SSPM used is the statistical model called Ordinary Kriging (OK); whose technique was developed by Krige (1951). The predictions are based on the model:

$$Z(s) = \mu + \varepsilon'(s) \quad (1)$$

Where μ is the constant stationary function (global mean) and $\varepsilon'(s)$ is the spatially correlated stochastic part of variation. The predictions are made as in Matheron (1963) and Gandin (1960) introduced to the analysis of point data is the derivation and plotting of the so-called semivariances — differences between the neighbouring values:

$$\gamma(h) = \frac{1}{2} E \left[(z(s_i) - z(s_i + h))^2 \right] \quad (2)$$

where $z(s_i)$ is the value of target variable at some sampled location and $z(s_i + h)$ is the value of the neighbour at distance $s_i + h$. The semivariances versus their distances produce a standard experimental variogram.

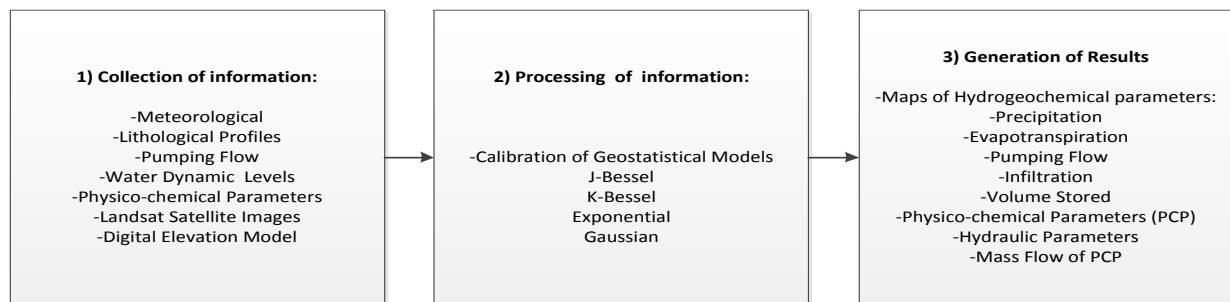


Fig. 2. Workflow for Spatio-Temporal Geostatistical Modeling of Hydrogeochemical Parameters in the San Diego Aquifer, Carabobo State, Venezuela.

Table: 1. Telemetric network of climate monitoring stations in the San Diego aquifer, Carabobo State, Venezuela.

Number	Projected Coordinates		Station Code	Station Name
	X	Y		
1	665682	1124668	AR01486AP1	SANTA CRUZ
2	648392	1140698	AR07241AP1	FORESTAL EL LIMON
3	670277	1121114	AR07330AP1	BELLA VISTA
4	653937	1133689	AR00456AS3	MARACAY- BASE ARAGUA
5	647690	1132951	AR80413AS3	MARACAY-BASE SUCRE-OMM
6	608178	1131078	CA00461AP1	VALENCIA-OFICINA
7	608490	1159760	CA80412AS4	PTO CABELLO BASE NAVAL
8	592724	1106863	CA01397AP1	CAMPO CARABOBO
9	616988	1138671	CA00451AP1	SAN DIEGO
10	622892	1135723	CA00423AP1	VIGIRIMA
11	613822	1154779	CA00412AP1	HDA EL MANGLAR
12	626026	1110365	CA00489AP1	AGUA BLANCA
13	598708	1124960	CA07346AP1	GUATAPARO CAMPO DE GOLF
14	619290	1112277	CA07297AP1	PLANTA DE POTABILIZACION
15	622148	1131688	CA00452AP1	GUACARA
16	603183	1134833	CA01310AP1	GUAPARO-EL CAFÉ
17	578351	1138895	CA01370AP1	CANOABO
18	630433	1102181	CA02404AP1	MANUARE
19	608661	1136374	CA07332AP1	UNIVERSIDAD DE CARABOBO
20	658047	1108591	CA07331AP1	LA CENIZA
21	616524	1122118	CA80472AS3	VALENCIA-AEROPUERTO
22	822700	1145984	MI01448AP1	LOS TEQUES INOS
23	726392	1144229	MI00561AP1	SAN DIEGO-MIRANDA
24	735254	1160195	MI80416AS3	CARACAS LA CARLOTA-OMM
25	726854	1151375	MI00563AC1	CARACAS LA MARIPOSA
26	595605	1078264	CO02349AP1	PAO OFICINA
27	546523	1066369	CO07320AS3	SAN CARLOS AEROPUERTO
29	677610	1097000	GU02417AS3	SAN JUAN DE LOS MORROS
30	617013	1160036	DC07315AP1	CARACAS UNEXPO
31	729293	1156854	DC07335AP1	FUERTE TIUNA

RESULTS

Geophysical parameters

The soil of the San Diego aquifer is composed by mineral particles classified according to the Unified Soil Classification System (USCS) on a sample of twenty eight lithological profiles extracted from pumping wells indicated in the Figure 3. In this sample of soil profiles, there are the following materials arranged

in a varied form regarding the type of material and thickness of the soil layer: GW: well-graded gravel, GC: clayey gravel, GM: silty gravel, SW: well-graded sand, SM: silty sand, SC: clayey sand, CL: clay of low plasticity, ML: silt, VL: vegetation layer, R: Rock. In the north region, the materials mainly constitute the profile integrated by: GW and CL. In the middle and south region, the profile

contains alternating layers of fine material such as: SW and CL. The depth of pumping wells varies between 43 and 175 mbgs (Table 2). According to the location

of the impervious layer constituted by CL with respect to the layers of GM, GC, SW or SM, the type of aquifer is confined.

Table: 2. Lithological profile into the San Diego aquifer shown in Figure 2.

a	b	c	d	a	b	c	d	a	b	c	d	a	b	c	d	a	b	c	d	a	b	c	d						
1	0	1	VL	2	0	1	VL	3	0	2	VL	4	0	1	VL	5	0	1	VL	6	0	0.5	VL	7	0	0.5	VL		
1	1	12	SM	2	1	8	GW	3	2	23	CL	4	1	16	CL	5	1	9	GW	6	0.5	5	SC	7	0.5	5	SM		
1	12	50	SW	2	8	12	CL	3	23	33	GW	4	16	32	SW	5	9	22	ML	6	5	7	CL	7	5	7	CL		
1	50	62	GW	2	12	18	GW	3	33	53	GC	4	32	47	GW	5	22	44	GW	6	7	19	SM	7	7	18	SM		
1	62	83	SW	2	18	34	CL	3	53	54	SM	4	47	58	R	5	44	59	R	6	19	23	SM	7	18	21	CL		
				2	34	42	SM	3	54	60	CL									6	23	31	CL	7	21	42	SW		
				2	42	47	GW	3	60	71	GC									6	31	34	SW	7	42	44	SW		
				2	47	73	GC													6	34	56	CL	7	44	93	SM		
				2	73	94	CL													6	56	58	SM	7	93	96	CL		
																				6	58	73	CL	7	96	102	GM		
																				6	73	77	SM	7	102	105	CL		
																				6	77	98	CL	7	105	108	GM		
																				6	98	101	SM	7	108	110	CL		
																				6	101	105	CL	7	110	119	GM		
																				6	105	109	SM	7	119	128	CL		
																				6	109	122	CL	7	128	139	GM		
																				6	122	128	SM	7	139	142	CL		
																				6	128	133	CL	7	142	150	GM		
																				6	133	139	SM	7	150	153	SW		
																				6	139	142	CL	7	153	160	CL		
																				6	142	147	SM						
																				6	147	150	CL						
																				6	150	162	SM						
																				6	162	170	CL						
																				6	170	173	SM						
																				6	173	175	CL						
a	b	c	d	a	b	c	d	a	b	c	d	a	b	c	d	a	b	c	d	a	b	c	d	a	b	c	d		
8	0	0.5	VL	9	0	17	CL	10	0	5	SC	11	0	2	VL	12	0	18	VL	13	0	1	VL	14	0	18	VL		
8	0.5	5	SC	9	17	52	SC	10	5	7	CL	11	2	23	CL	12	18	24	SW	13	1	22	CL	14	18	36	SW		
8	5	7	CL	9	52	67	GW	10	7	12	SW	11	23	33	GC	12	24	42	SW	13	22	25	SW	14	36	48	GW		
8	7	20	SC	9	67	77	GM	10	12	20	CL	11	33	52	GW	12	42	48	SM	13	25	44	CL	14	48	72	SW		
8	20	25	SW	9	77	105	CL	10	20	26	SC	11	52	54	SM	12	48	54	CL	13	44	50	SW	14	72	78	CL		
8	25	56	CL	9	105	112	ML	10	26	53	CL	11	54	60	CL	12	54	60	CL	13	50	59	GW	14	78	92	CL		
8	56	64	SC	9	112	117	CL	10	53	65	CL	11	60	76	GC	12	60	66	SW	13	59	85	CL						
8	65	75	CL	9	117	126	ML	10	65	81	CL								12	66	72	CL	13	85	90	CL			
8	75	83	SW	9	126	136	SM	10	81	83	SW								12	72	96	SW							
8	83	108	CL	9	136	156	SW	10	83	110	SC																		
8	108	115	SW	9	156	160	CL	10	110	119	SC																		
8	115	127	SC						119	123	CL																		
8	127	133	SW						123	139	SW																		
8	133	138	CL						139	141	CL																		
8	138	146	SW																										
8	146	150	CL																										
15	0	1	VL	16	0	6	VL	17	0	0.5	VL	18	0	1	VL	19	0	1	VL	20	0	12	VL	21	0	1	VL		
15	1	16	CL	16	6	19	SM	17	0.5	5	SM	18	1	6	SW	19	1	14	CL	20	12	42	SW	21	1	13	CL		
15	16	32	SW	16	19	37	SW	17	5	31	CL	18	6	9	SC	19	14	30	GW	20	42	60	GW	21	13	32	SW		
15	32	47	GW	16	37	49	GW	17	31	64	R	18	9	18	GW	19	30	40	CL	20	60	66	GC	21	32	43	GC		
15	47	58	R	16	49	61	SW					18	18	30	R	19	40	60	CL	20	66	81	SW	21					
				61	67		CL					18	30	66	R	19	60	80	GW										
				67	82		SW																						
a	b	c	d	a	b	c	d	a	b	c	d	a	b	c	d	a	b	c	d	a	b	c	d	a	b	c	d		
22	0	33	SC	23	0	4	VL	24	0	1	VL	25	0	9	SM	26	0	6	SM	27	0	1	VL	28	0	2	VL		
22	33	45	SW	23	4	6	SC	24	1	9	SW	25	9	20	CL	26	6	9	CL	27	1	15	SW	28	2	4	CL		
22	45	51	CL	23	6	14	SW	24	9	22	CL	25	20	24	GW	26	9	15	SW	27	15	25	GW	28	4	26	SW		
22	51	63	SW	23	14	18	CL	24	22	32	CL	25	24	27	CL	26	15	21	GW	27	25	40	GC	28	26	34	SC		
22	63	69	CL	23	18	24	SW	24	32	44	GW	25	27	30	SW	26	21	24	CL	27	40	50	SW	28	34	36	SW		
22	69	81	SW	23	24	28	CL	24	44	59	R	25	30	34	GW	26	24	27	SW	27	50	70	GW	28	36	42	CL		
22	81	87	CL	23	28	30	GW					25	34	37	CL	26	27	30	SM					28	42	50	SC		
22	87	99	GW	23	30	32	SW					25	37	40	SW	26	30	36	SW					28	50	54	SW		
22	99	105	CL	23	32	34	CL					25	40	44	GW	26	36	39	CL					28	54	70	CL		
22	105	117	SW	23	34	44	GW					25	44	51	SW	26	39	50	GW					28	70	90	SC		
				23	44	48	CL																		28	90	98	CL	
				23	48	52	SW																		28	98	104	SC	
				23	52	54	CL																		28	104	108	CL	
				23	54	56	SW																						
				23	56	60	CL																						
				23	60	66	SC																						
				23	66	68	CL																						
				23	68	70	SW																						
				23	70	72	CL																						
				23	72	74	SC																						
				23	74	78	CL																						
				23	78	84	SW																						
				23	84	86	CL																						
				23	86	88	SW																						
				23	88	94	CL																						

a: number of lithological profile, b: upper limit of layer, c: lower limit

Classification System (USCS) as: GW: well-graded gravel, GC: clayey gravel, GM: silty gravel, SW: well-graded sand, The profiles of effective porosity and permeability show that these vary according to the material (Figure 4, Figure 5), for GW and SW: 0.38 and 0.4, CL: 0.10; with respect to the permeability: GW: 1000 m/d, GC, GM, SW: 100 m/d,

SM: silty sand, SC: clayey sand, CL: clay of low plasticity, ML: silt, VL: vegetation layer, R: Rock.

SM, SC: 10 m/d, CL, ML: 0.1 m/d. In the aquifer zone, the effective porosity and permeability take high values by comparing with the impervious material such as SC, CL and ML.

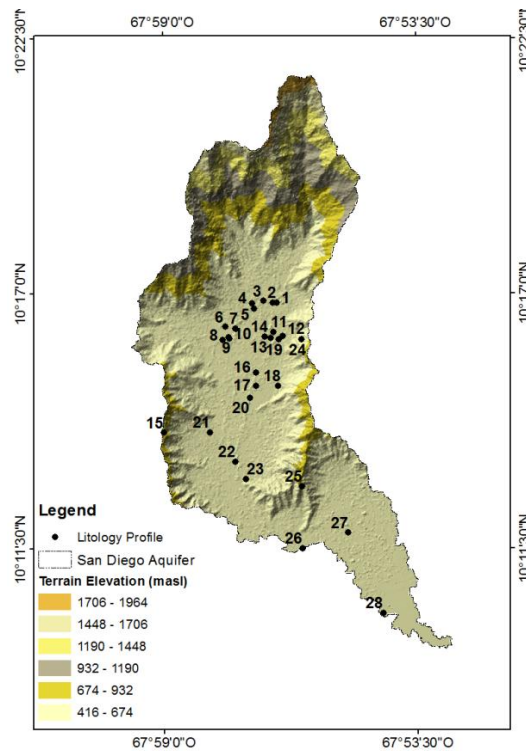


Fig. 3. Lithological profiles of pumping wells into the San Diego aquifer. The 28 lithological profiles are located between the following terrain elevations: 416 and 674 masl, and two between 674 and 932 masl.

Land Use / Land Cover

The spatial distribution of land use and land cover in the aquifer of San Diego to month scale during the period between 2015 and 2018 is shown in Figure 6. The total area of the aquifer is 116 km². The Figure 7 shows the accumulated area by including the area corresponds to the land use and land cover on the San Diego aquifer. The vegetation covers in the north region permanently, varying between 18.21 and 71.96 km² (15.7 and 62%) according to the season into the year

(Figure 7). The vegetation area contributes to the recharge of groundwater because of infiltration and inflow through the domains boundaries. The degraded soil zone covers the central region, varying between 6.54 and 44.48 km² (5.6 and 38.34 %). The urban zone covers the central region, varying between 24.09 and 56.47 km² (20.76 and 48.6%). The agricultural zone is distributed between central and south region, varying between 0 and 30.22 km² (0 and 26%).

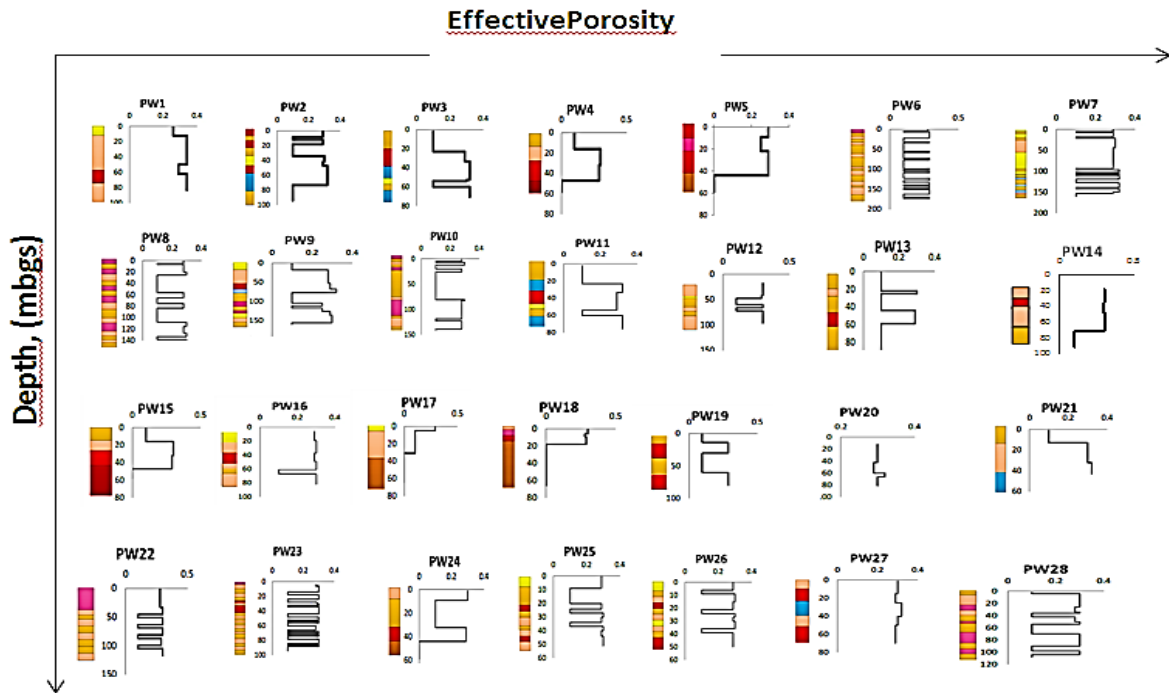


Fig. 4. Profiles of effective porosity of pumping wells into the San Diego aquifer. The 26 lithological profiles are located between the following terrain elevations: 416 and 674 masl, and two between 674 and 932 masl.

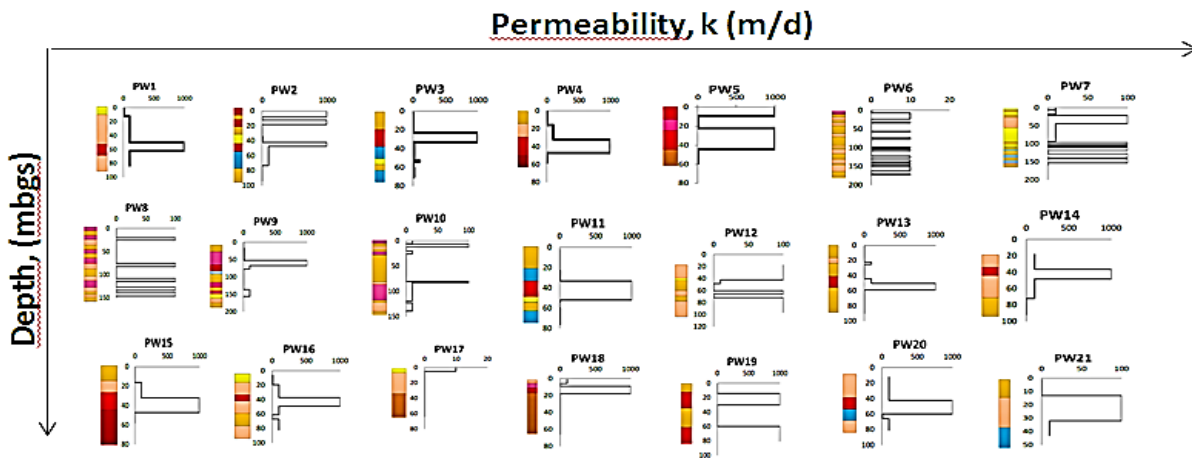


Fig. 5. Profiles of permeability of pumping wells into the San Diego aquifer. The 26 lithological profiles are located between the following terrain elevations: 416 and 674 masl, and two between 674 and 932 masl.

Groundwater Balance

1) *Precipitation:* the monthly precipitation in a way of rainfall is spatially distributed in a low intensity in the north and central region regarding to the south region of the San Diego aquifer during the dry season (Figure 8). In the north and central region, the precipitation varies between 0 and 21 mm/month during the dry season. In the south region, the precipitation varies

between 4 and 44 mm/month during the dry season. The monthly precipitation in the north and central region varies between 28 and 291 mm/month during the rainy season. In the south region, the precipitation varies between 61 and 311 mm/month during the rainy season. The statistical spatial prediction model (SSPM) is the J-Bessel function. This function is fitted to the observed precipitation with a

gradient that varies between 0.3 and 0.7. The equation is identified by the following coefficients in a general structure: $a \cdot \text{nugget} + b(\text{J-Bessel}(c, d))$. The values of coefficients vary as follows (Table 3): a : between 0 and 5905, b : between 14.513 and 5933, c : between 25056 and 995790, d : between 0.01 and 5.37. The coefficient a is associated with the no spatial correlation. The coefficient b is associated with $C_0 + C_1$ term, which is the sill variation. The coefficient c represents the maximum distance between stations of neighbor precipitation observations. The coefficient d represents the parameter of the J-Bessel function. There is pattern in the SPPMs for the dry season, associated with the first months of the each year. In all cases, the semivariences are smaller at shorter distance and then they stabilize at some distance.

2) *Evapotranspiration*: the monthly evapotranspiration is spatially distributed in a high intensity in the north and central region regarding to the south region of the San Diego aquifer during the dry season (Figure 9). In the north and central region, the evapotranspiration varies between 64 and 188 mm/month during the dry season. In the south region, the precipitation varies between 29 and 185 mm/month during the dry season. The monthly evapotranspiration in the north and central region varies between 86 and 141 mm/month during the rainy season. In the south region, the monthly evapotranspiration varies between 85 and 137 mm/month during the rainy season. The statistical spatial prediction model (SSPM) is the J-Bessel function. This function is fitted to the observed precipitation with a gradient that varies between 0.24 and 0.65. The equation is identified by the following coefficients in a general structure: $a \cdot \text{nugget} + b(\text{J-Bessel}(c, d))$. The values of coefficients vary as follows (Table 4): a : between 0 and 683, b : between 5.2 and 3673.6, c : between 57392 and 1674300, d : between 0.01 and 10.

There is pattern in the SPPMs for the dry and rainy seasons.

3) *Pumping flow*: the monthly pumping flow is spatially distributed with a high intensity in the central and south regions regarding to the north region of the San Diego aquifer under a stationary regime (Figure 10). In the north region, the pumping flow varies between 0 and 6 l/s. In the central and south regions, the pumping flow varies between 6 and 20 l/s. The statistical spatial prediction model (SSPM) is the J-Bessel function. This function is fitted to the observed pumping flow with a gradient that varies between 0.55 and 0.57. The equation is identified by the following coefficients in a general structure: $a \cdot \text{nugget} + b(\text{J-Bessel}(c, d))$. The values of coefficients vary as follows (Table 5): a : between 9.04 and 10.28, b : between 57.13 and 78.1, c : between 20205 and 25980, d : between 1.2271 and 1.6849. There is permanent pattern in the SPPMs. The forecast model of a , c and d coefficients of SSPM is ARIMA (1,0,1).

4) *Infiltration*: the monthly infiltration is spatially distributed with a high intensity in the north and central region regarding to the south region of the San Diego aquifer during the dry season (Figure 11). In the north and central region, the infiltration varies between 0 and 11 mm/month during the dry season. In the south region, the infiltration varies between 1 and 15 mm/month during the dry season. The infiltration in the north and central region varies between 20 and 113 mm/month during the rainy season. In the south region, the infiltration varies between 34 and 126 mm/month during the rainy season. The statistical spatial prediction model (SSPM) is the J-Bessel function. This function is fitted to the observed infiltration with a gradient that varies between 0.24 and 0.65. The equation is identified by the following coefficients in a general structure: $a \cdot \text{nugget} + b(\text{J-Bessel}(c, d))$. The values of coefficients vary as follows (Table 6): a : between 0 and 103, b :

between 0.00037546 and 197.53, c: between 143.68 and 10781, d: between 0.1298 and 10. There is pattern in the SPPMs for the dry and rainy seasons.

5) *Volume Stored*: the monthly volume stored is spatially distributed with a high intensity in the north and central region regarding to the south region of the San Diego aquifer permanently (Figure 12). In the north and central mountainous region, the volume stored expressed as mm/month varies between -96 and 6 mm; being the month of august, when the volume stored is the minimum. The monthly volume stored varies between -48 and -9 mm during the dry season. The monthly volume stored varies between 21 and 26 mm during the rainy season. The statistical spatial prediction model (SSPM) is the J-Bessel function. This function is fitted to the observed monthly volume stored with a gradient that varies between 0.87 and 0.99. The equation is identified by the following coefficients in a general structure: $a \cdot \text{nugget} + b(\text{J-Bessel}(c, d))$. The values of coefficients vary as follows (Table 7): a: between 0 and 103, b: between 0.00037546 and 197.53, c: between 143.68 and 10781, d: between 0.1298 and 10. There is pattern in the SPPMs for the dry and rainy seasons.

Physico-Chemical Parameters

The physico-chemical parameters in the water pumped from the San Diego aquifer measured during the period between 2015-2017 are the following a) Bicarbonate (mg/l) b) Chloride (mg/l), c) Sulfate (mg/l), d) Nitrate (mg/l), e) Calcium (mg/l), f) Magnesium (mg/l), g) Sodium (mg/l), h) Potassium (mg/l), i) Dissolved Solids (mg/l), j) Temperature (°C), k) Electrical conductivity (µS/cm), l) pH, m) Alkalinity (mg/l CaCO₃), n) Total Hardness (mg/l CaCO₃), o) Calcic hardness (mg/l CaCO₃), p) Magnesium hardness (mg/l CaCO₃). (Figure 13, Table 32). The bicarbonate varies between 81 and 333 mg/l, Chloride between 5 and 81

mg/l, Sulfate between 0 and 461 mg/l, Nitrite between 0 and 18 mg/l, Calcium between 0 and 119 mg/l, Magnesium between 6 and 45 mg/l, Sodium between 0 and 219 mg/l, Potassium between 0 and 17 mg/l, Dissolved Solids between 87 and 1384 mg/l, Temperature between 27 and 28 °C, Electrical conductivity between 188 and 2341 µS/cm, pH between 6 and 8, Alkalinity between 91 and 318 mg/l CaCO₃, Total hardness between 52 and 618 mg/l CaCO₃, Calcic hardness between 0 and 295 mg/l CaCO₃, Magnesium hardness between 22 and 232 mg/l CaCO₃. In the north and central region of the San Diego aquifer the physico-chemical parameters take the minimum values. The whole of the physico-chemical parameters measured take the maximum values to the south zone of the San Diego aquifer in the boundary with the Valencia Lake, where the land use corresponds to urban and agricultural. According to the Sanitary Standards of Quality of Drinking Water published by the Ministry of Health and Social Assistance in the Official Gazette of the Republic of Venezuela with the number 36.395, the threshold of the physico-chemical parameters is as follows: Chloride < 300 mg/l, pH < 9, Sulfate < 500 mg/l, Total hardness < 500 mg/l CaCO₃, Dissolved Solids < 1000 mg/l, Nitrite between < 0.03 mg/l, Sodium < 200 mg/l. The quality of water in the north zone of San Diego aquifer is acceptable for human consumption, while in the south zone, the water quality is slightly upper than the threshold of the environmental regulation in most of the physico-chemical parameters. The water of the Valencia Lake is contaminated; this contamination has its origin in the discharges of sewage from domestic and industrial sources and, to a lesser extent, agricultural activities (Guevara, 2000). According to values reported in recent studies (IESA, 1998), the lake has a characteristic of hyper-eutrophication in areas near the outlets of its main rivers.

From these results, it can be supposed that the water quality of the Valencia Lake is causing the increase of the physico-chemical parameters of water quality of San Diego aquifer because of water recharge from the Valencia Lake to the groundwater of the San Diego aquifer during the dry season. The statistical spatial prediction model (SSPM) for whole of physico-chemical parameters is the J-Bessel function. This function is fitted to the observed physico-chemical parameters with a gradient that varies between 0.12 and 0.54 (Table 8). The equation is identified by the following coefficients in a general structure: $a \cdot \text{nugget} + b(\text{J-Bessel}(c, d))$. The values of coefficients vary according to the neighbors values in each dataset of physico-chemical parameters, as a sample, the coefficients for the alkalinity SSPM are as follows (Table 8): a: 4349.1, b: 4949.9, c: 22035, d: 0.11652.

Hydraulic Parameters

The hydraulic parameters from the San Diego aquifer measured during the period between 2015-2017 are the following: water dynamic level (Figure 14, Table 33), hydraulic gradient (Figure 15, Table 34) and flow velocity (Figure 16). The water dynamic level varies during the period 2015-2017 as follows: for 2015: between 385 and 574 masl, for 2016: between 329 and 803 masl, for 2017: between 329 and 803 masl. The highest elevations measured of the water dynamic level, trend to occur at the end of the mountain chain located to the south region of San Diego aquifer. The lowest elevations measured of the water dynamic level, trend to occur at the plains of the center and south regions of the aquifer. The statistical spatial prediction model (SSPM) for whole of water dynamic levels measured during the period 2015-2017 is the J-Bessel function. This function is fitted to the observed water dynamic level with a gradient that varies between 0.88 and 0.98 (Table 9). The equation is identified by the following

coefficients in a general structure: $a \cdot \text{nugget} + b(\text{J-Bessel}(c, d))$. The values of coefficients vary according to the neighbors values in each dataset of water dynamic levels, as a sample, the coefficients for the water dynamic levels for 2015 are as follows (Table 9): a: 1281.6, b: 5000.7, c: 14136, d: 10.

The hydraulic gradient varies during the period 2015-2017 as follows: for 2015: between 0 and 39 %, for 2016: between 0 and 29%, for 2017: between 0 and 55%. The highest hydraulic gradient estimated of the groundwater, trend to occur at the two regions following: 1) in the central region and 2) at the end of the mountain chain located to the south region of San Diego aquifer. In the central region, the gradient is explained by two reasons: the pumping wells N° 6 to N° 10 where it is found high frequency of clay of low plasticity layers varying between 7 and 11 layers for the greatest deeps in the aquifer, which vary between 141 and 173 masl (Figure 3, Table 3). 2) a possible lack of well maintenance of the metal grid located in the aquifer layer composed by well-graded gravel (GW) and well-graded sand (SW) occluding the water inlet to the well. The statistical spatial prediction model (SSPM) for whole of hydraulic gradients estimated during the period 2015-2017 is the J-Bessel function. This function is fitted to the observed hydraulic gradient with a gradient that varies between 0.77 and 0.94 (Table 10). The equation is identified by the following coefficients in a general structure: $a \cdot \text{nugget} + b(\text{J-Bessel}(c, d))$. The values of coefficients vary according to the neighbors values in each dataset of hydraulic gradient, as a sample, the coefficients for the water dynamic levels for 2015 are as follows (Table 10): a: 2.0954, b: 6.1085, c: 795.48, d: 10.

The flow velocity varies during the period 2015-2017 as follows: for 2015: between 0 and 2033 m/d, for 2016: between 0 and

946 m/d, for 2017: between 0 and 1259 m/d. The highest flow velocity estimated of the groundwater, trend to occur at the north region of San Diego aquifer; trending to zero to the central and north region of the aquifer, indicating that this is the water recharge zone. The soil profile of the wells located in the north region close to the mountains contain between 1 and 4 layers of well-graded gravel (GW) and clayey gravel (GC) as it is shown in Table 1; where the effective porosity and the permeability take the maximum values as 0.4 and 1000 m/d, respectively (Figure 4, Figure 5).

Mass flow of physico-chemical parameters

The mass flow of physico-chemical parameters from the San Diego aquifer estimated during the period between 2015-2017 are the following (Figure 17): a) Alkalinity for 2015 varies between 91 and 1E06 kg/d, b) Alkalinity for 2016 varies between 17 and 456294 kg/d, c) Alkalinity for 2017 varies between 17 and 456294 kg/d, d) Chloride for 2015 varies between 17 and 456294 kg/d, e) Chloride for 2016 varies between 17 and 456294 kg/d, f) Chloride for 2017 varies between 1 and 99757 kg/d, g) Sulfate for 2015 varies between 17 and 456294 kg/d, h) Sulfate for 2016 varies between 0 and 88514 kg/d, i) Sulfate for 2017 varies between 0 and 149459 kg/d, j) Total Hardness for 2015 varies between 59 and 962123 kg/d, k) Total Hardness for 2016 varies between 16 and 383595 kg/d, l)

Total Hardness for 2017 varies between 46 and 474531 kg/d, m) Nitrite for 2015 varies between 0 and 6800 kg/d, n) Nitrite for 2016 varies between 0 and 2117 kg/d, o) Nitrite for 2017 varies between 0 and 2772 kg/d, p) Sodium for 2015 varies between 3 and 153160 kg/d, q) Sodium for 2016 varies between 1 and 72383 kg/d, r) Sodium for 2017 varies between 1 and 103108 kg/d, s) Potassium for 2015 varies between 0 and 13285 kg/d, t) Potassium for 2016 varies between 0 and 18103 kg/d, u) Potassium for 2017 varies between 0 and 11655 kg/d, v) Calcium for 2015 varies between 0 and 170899 kg/d, w) Calcium for 2016 varies between 0 and 73035.5 kg/d, x) Calcium for 2017 varies between 0 and 98479.3 kg/d. In general, the flow mass follows the pattern observed in the representation of the flow velocity, the highest flow velocity occurs in the north region where the mountains are located. The statistical spatial prediction model (SSPM) for the mass flow estimated during the period 2015-2017 is the J-Bessel function. This function is fitted to the observed water dynamic level with a gradient that varies between 0.88 and 0.98 (Table 11). The equation is identified by the following coefficients in a general structure: $a \cdot \text{nugget} + b \cdot \text{J-Bessel}(c, d)$. The values of coefficients vary according to the neighbors values in each dataset of mass flow, as a sample, the coefficients for the mass flow of alkalinity as CaCO_3 for 2015 are as follows (Table 11): a: 9.6802e8, b: 1.3745e9, c: 569.2, d: 10.

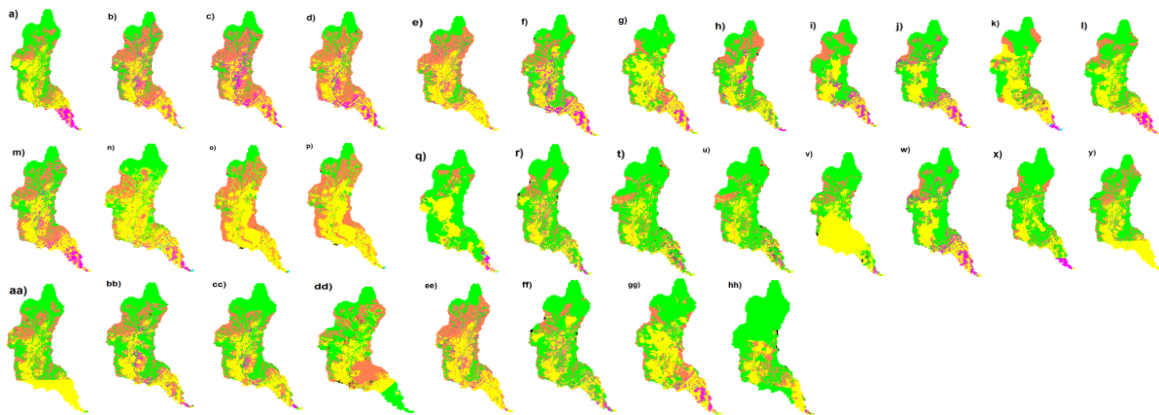


Fig. 6. Land use and land cover in the Pao river basin in the month period between January 2015 and July 2017

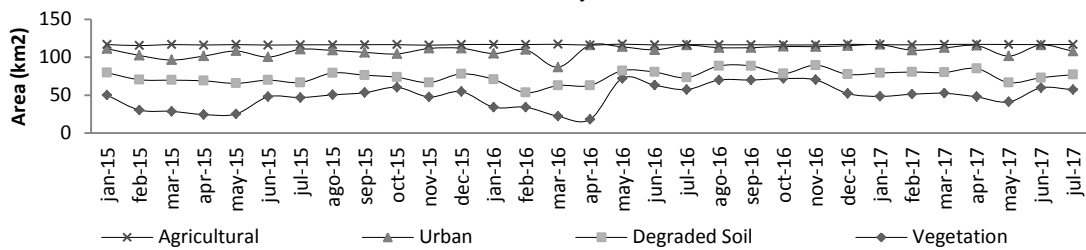
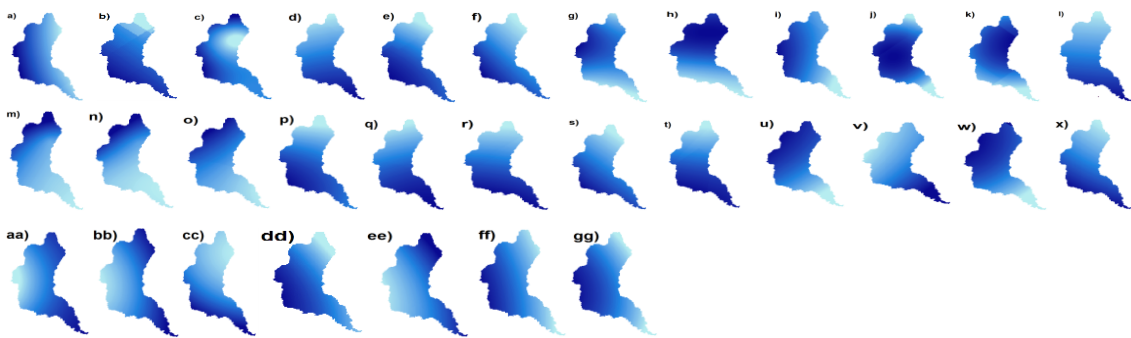


Fig. 7. Distribution of Area for land use and land cover in the San Diego aquifer in the month period between January 2015 and July 2017



	a	b	c	d	e	f	g	h	i	j	k	l
Min.	3	6	0	21	35	25	106	168	28	74	50	18
Máx.	5	11	4	44	74	61	167	403	178	132	77	22

	m	n	o	p	q	r	s	t	u	v	w	x
Min.	0	0	0	131	102	121	153	103	248	113	275	18
Máx.	1	1	4	201	165	239	168	223	331	142	311	21

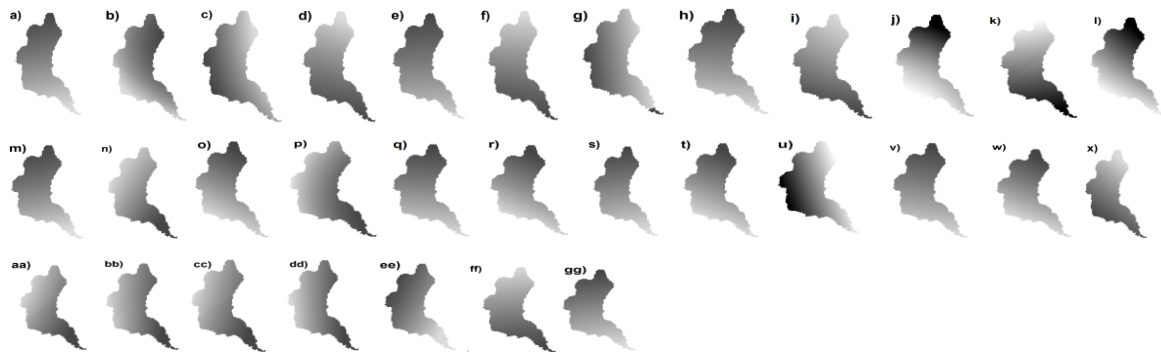
	y	z	aa	bb	cc	dd	ee
Min.	7	0	11	197	114	291	270
Máx.	12	12	15	202	126	298	275

Fig. 8. Spatial prediction of the monthly precipitation (mm/month) that occurred over the aquifer of San Diego Municipality during the period 2015-2017: Figure 8a - l: January-December 2015, Figure 8 m-x: January-December 2016, Figure 8 y-e: January - July 2017.

Table: 3. Results of Modelling of Statistical Spatial Prediction of the Monthly Precipitation based on the time series between 2015 and 2017 in the Aquifer of the Municipality of San Diego, Carabobo State.

Precipitation	Prediction Model	Ordinary Krigging
January 2015	SSPM	19.522*Nugget+159.2*J-Bessel(178510,2.0489)
	PRF	0.532238183609308 * x + 4.42873087404682
February 2015	SSPM	34.818*Nugget+158.49*J-Bessel(271440,4.8261)
	PRF	0.531523366999772 * x + 3.66653569087514
March 2015	SSPM	1.4603*Nugget+110.54*J-Bessel(210830,1.5538)
	PRF	0.501745953386823 * x + 2.15715565599625
April 2015	SSPM	23.597*Nugget+195.03*J-Bessel(44358,5.3761)
	PRF	0.529218165970819 * x + 8.67733392322315
May 2015	SSPM	118.21*Nugget+236.64*J-Bessel(53709,0.43129)
	PRF	0.485604025574778 * x + 22.6873098318075
June 2015	SSPM	26.471*Nugget+406.8*J-Bessel(56331,0.01)
	PRF	0.543249555081704 * x + 23.5392157470299
July 2015	SSPM	0*Nugget+2851*J-Bessel(26398,2.8903)
	PRF	0.571765407138565 * x + 41.5040609865655
August 2015	SSPM	0*Nugget+14715*J-Bessel(32097,0.70572)
	PRF	0.662375738328587 * x + 50.7422696548426
September 2015	SSPM	0*Nugget+3627.1*J-Bessel(23952,1.7193)
	PRF	0.535257009807157 * x + 30.4980732273241
October 2015	SSPM	0*Nugget+2768.7*J-Bessel(40582,0.32488)
	PRF	0.709069196192058 * x + 21.5079966399872
November 2015	SSPM	38.461*Nugget+730.34*J-Bessel(53709,0.01)
	PRF	0.859862882143079 * x + 8.2531093267537
December 2015	SSPM	132.74*Nugget+1042.9*J-Bessel(995790,0.01)
	PRF	0.405731993270988 * x + 10.8261034031106
January 2016	SSPM	0*Nugget+30.567*J-Bessel(158760,1.8769)
	PRF	0.726258891796951 * x + 0.831321120960159
February 2016	SSPM	5.1545*Nugget+88.619*J-Bessel(329260,1.8517)
	PRF	0.726209572574087 * x + 1.13799503039787
March 2016	SSPM	0*Nugget+14.513*J-Bessel(59080,0.01)
	PRF	0.43968759952042 * x + 0.533756430796383
April 2016	SSPM	831.58*Nugget+1898.5*J-Bessel(47718,0.01)
	PRF	0.451890263420529 * x + 72.3163761825868
May 2016	SSPM	516.66*Nugget+1268.9*J-Bessel(56331,0.01)
	PRF	0.422633713944521 * x + 65.0572964189686
June 2016	SSPM	2828.6*Nugget+5413.6*J-Bessel(64988,0.047188)
	PRF	0.36257192747007 * x + 108.403000222451
July 2016	SSPM	1734.4*Nugget+3275.3*J-Bessel(314500,0.01)
	PRF	0.535251234426308 * x + 101.511441545499
August 2016	SSPM	285.48*Nugget + 3569.9*J-Bessel(53709,0.01)
	PRF	0.3487 * x + 98.25004
September 2016	SSPM	3580.9*Nugget+7951.1*J-Bessel(70621,2.0628)
	PRF	0.521018315209597 * x + 89.2153102915013
October 2016	SSPM	557.2*Nugget+1471.7*J-Bessel(107010,0.01)
	PRF	0.375497702273485 * x + 81.6411650714322
November 2016	SSPM	5905.5*Nugget+4061*J-Bessel(105590,0.01)
	PRF	0.363734912482319 * x + 119.023071628874
December 2016	SSPM	188.92*Nugget+739.86*J-Bessel(313770,0.01)
	PRF	0.432390024159167 * x + 20.1213030430473
January 2017	SSPM	7.2046*Nugget + 294.95*K-Bessel(25056,0.81312)
	PRF	0.5435 * x + 10.0861874396207
February 2017	SSPM	0*Nugget + 212.95*J-Bessel(37917,0.01)
	PRF	0.5157 * x + 5.3918
March 2017	SSPM	267.05*Nugget+844.75*J-Bessel(233170,0.01)
	PRF	0.353951048927083 * x + 23.4768407446735
April 2017	SSPM	232.82*Nugget + 2080.3*J-Bessel(194470,0.01)
	PRF	0.2216 * x + 87.9910
May 2017	SSPM	94.699*Nugget+1346.9*J-Bessel(201320,0.01)
	PRF	0.304747671720388 * x + 86.5815975679705
June 2017	SSPM	3874.2*Nugget + 3889.7*J-Bessel(185810,1.2106)
	PRF	0.34858 * x + 140.7880
July 2017	SSPM	4830.6*Nugget + 5933.1*J-Bessel(186820,1.2692)
	PRF	0.36677 * x + 114.529437006694

SSPM: Statistical Spatial Prediction Model, PRF: Predicted Regression function,

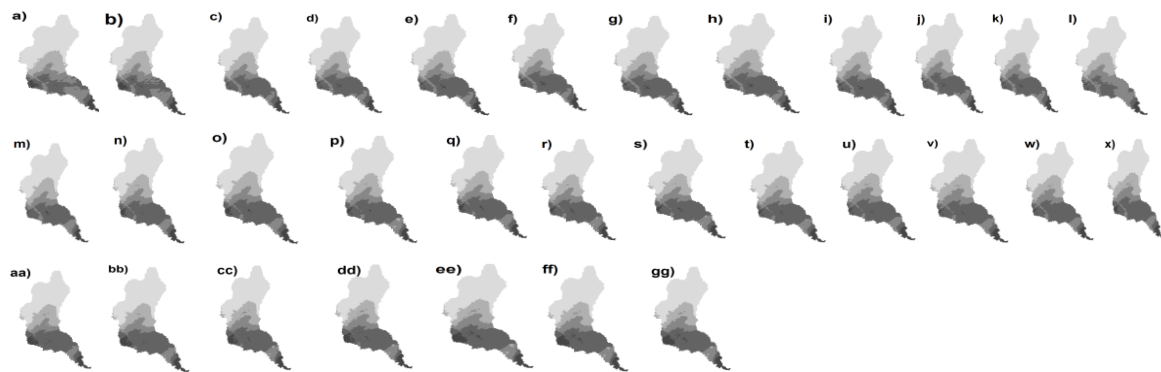


	a	b	c	d	e	f	g	h	i	j	k	l
Min.	115	170	151	157	162	123	128	137	117	132	137	109
Máx.	123	174	155	158	167	128	132	147	119	134	143	115

	m	n	o	p	q	r	s	t	u	v	w	x
Min.	141	137	185	138	117	122	142	122	98	121	85	90
Máx.	142	138	188	141	122	125	144	125	103	125	86	91

	y	z	aa	bb	cc	dd	ee
Min.	29	80	105	85	108	116	122
Máx.	64	90	124	97	113	121	123

Fig: 9. Spatial prediction of the monthly evapotranspiration (mm/month) that occurred over the aquifer of San Diego Municipality during the 2015-2017 period: Figure 9a - l: January-December 2015, Figure 9m-x: January-December 2016, Figure 9y-e: January - July 2017.



	a	b	c	d	e	f	g	h	i	j	k	l
Min.	0	0	0	0	0	0	0	0	0	0	0	0
Máx.	19	19	19	19	19	19	19	19	19	19	19	19

	m	n	o	p	q	r	s	t	u	v	w	x
Min.	0	0	0	0	0	0	0	0	0	0	0	0
Máx.	19	19	19	19	19	19	19	19	19	19	19	19

	y	z	aa	bb	cc	dd	ee
Min.	0	0	0	0	0	0	0
Máx.	20	20	20	20	20	20	20

Fig: 10. Spatial prediction of the monthly pumping flow (l/s) that occurred over the aquifer of San Diego Municipality during the 2015-2017 period: Figure 10a - l: January-December 2015, Figure 10m-x: January-December 2016, Figure 10y-e: January - July 2017.

Table: 4. Results of Modelling of Statistical Spatial Prediction of the Monthly Evapotranspiration based on the time series between 2015 and 2017 in the Aquifer of the Municipality of San Diego, Carabobo State.

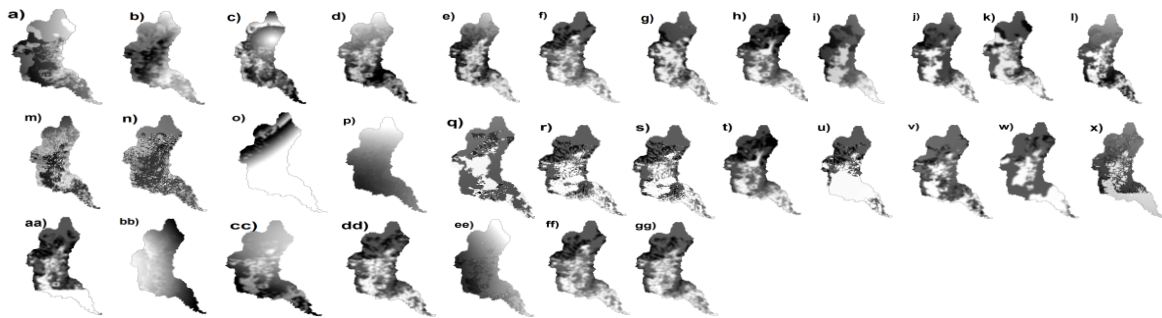
Evapotranspiration	Models	Ordinary Krigging
January 2015	SSPM	131.04*Nugget+3673.6*J-Bessel(1115100,0.51397)
	PRF	0.648144684643057 * x + 44.8318716808285
February 2015	SSPM	26.814*Nugget+835.17*J-Bessel(189670,0.49692)
	PRF	0.416364435864507 * x + 73.584673262016
March 2015	SSPM	89.766*Nugget+659.11*J-Bessel(419760,10)
	PRF	0.289067209546218 * x + 103.401744641693
April 2015	SSPM	683.27*Nugget+2433.1*J-Bessel(837650,0.19588)
	PRF	0.418465402182432 * x + 72.846971262649
May 2015	SSPM	677.73*Nugget+1097.1*J-Bessel(1104800,0.17348)
	PRF	0.308536599665459 * x + 109.010056119058
June 2015	SSPM	507.84*Nugget+659.26*J-Bessel(357190,0.045011)
	PRF	0.499550385080068 * x + 55.9044687903299
July 2015	SSPM	72.522*Nugget+1595.6*J-Bessel(433340,6.6714)
	PRF	0.514457004661164 * x + 59.9951416767641
August 2015	SSPM	300.57*Nugget+1560.1*J-Bessel(337540,3.8891)
	PRF	0.519745957176195 * x + 62.7979339208845
September 2015	SSPM	84.001*Nugget+606.38*J-Bessel(328480,0.21383)
	PRF	0.440529961125831 * x + 81.3847971636071
October 2015	SSPM	100.93*Nugget+636.1*J-Bessel(616450,7.6867)
	PRF	0.402862107527901 * x + 77.835331876368
November 2015	SSPM	29.762*Nugget+1504.5*J-Bessel(493500,1.6511)
	PRF	0.586373214151667 * x + 41.9363699462318
December 2015	SSPM	6.7862*Nugget+897.98*J-Bessel(276050,0.01)
	PRF	0.652092696696923 * x + 43.1883763030934
January 2016	SSPM	25.41*Nugget+147.81*J-Bessel(640110,0.01)
	PRF	0.606574268874103 * x + 52.5646550558943
February 2016	SSPM	50.958*Nugget+820.86*J-Bessel(576190,0.01)
	PRF	0.425546455395108 * x + 75.0265716584644
March 2016	SSPM	383.7*Nugget+1125.8*J-Bessel(809450,0.069314)
	PRF	0.511460801790995 * x + 81.3187313879988
April 2016	SSPM	66.79*Nugget+472.82*J-Bessel(175960,0.01)
	PRF	0.517198103028205 * x + 59.7907894634429
May 2016	SSPM	544.59*Nugget+2779.3*J-Bessel(1495900,0.01)
	PRF	0.496469645128778 * x + 56.6210390938054
June 2016	SSPM	454.16*Nugget+1579.9*J-Bessel(920530,0.23501)
	PRF	0.544958507204842 * x + 52.2452100084431
July 2016	SSPM	0*Nugget+156.85*J-Bessel(361330,0.01)
	PRF	0.547061432183571 * x + 65.1935275619968
August 2016	SSPM	457.58*Nugget+3812.9*J-Bessel(57392,0.01)
	PRF	0.237744317274072 * x + 132.879894776294
September 2016	SSPM	875.24*Nugget+2093.3*J-Bessel(537350,0.01)
	PRF	0.437168668133696 * x + 61.0411283732782
October 2016	SSPM	44.13*Nugget+1077.6*J-Bessel(807180,10)
	PRF	0.53483301523759 * x + 57.51928145705
November 2016	SSPM	27.944*Nugget+43.078*J-Bessel(896040,0.01)
	PRF	0.151289289956767 * x + 73.5036117426325
December 2016	SSPM	1.116*Nugget+5.2092*J-Bessel(1119900,10)
	PRF	0.339562300412332 * x + 59.7123877816331
January 2017	SSPM	0*Nugget+1454.4*J-Bessel(348960,0.01)
	PRF	0.367191150290792 * x + 87.4054993937792
February 2017	SSPM	0*Nugget+2191.4*J-Bessel(287670,0.13157)
	PRF	0.241741119572014 * x + 69.9514440235173
March 2017	SSPM	0*Nugget+4904.3*J-Bessel(404920,10)
	PRF	0.382304965087937 * x + 81.2556034373932
April 2017	SSPM	0*Nugget+2895.7*J-Bessel(289230,0.79683)
	PRF	0.439171522881292 * x + 58.5641155446115
May 2017	SSPM	0*Nugget+853.12*J-Bessel(704130,0.01)
	PRF	0.662843928659694 * x + 33.9482360629718
June 2017	SSPM	17.219*Nugget+2233.5*J-Bessel(1674300,10)
	PRF	0.699152931433195 * x + 43.0269990160359
July 2017	SSPM	129.05*Nugget+779.39*J-Bessel(704130,0.01)
	PRF	0.547168253081016 * x + 59.7716031267275

SSPM: Statistical Spatial Prediction Model, PRF: Predicted Regression function,

Table: 5. Results of the application of the ordinary krigging space prediction model of the monthly pumping flow on the aquifer of San Diego Municipality, Carabobo State.

Month	SSPM	Ordinary Krigging
January 2015	SSPM	9.5403*Nugget+62.577*J-Bessel(25571,1.4722)
	PRF	0.556118740851363 * x + 1.18158774020576
February 2015	SSPM	9.647*Nugget+62.604*J-Bessel(25980,1.3762)
	PRF	0.551860056019546 * x + 1.17686109803643
March 2015	SSPM	9.279*Nugget+62.96*J-Bessel(25843,1.4234)
	PRF	0.553711347716352 * x + 1.18949768295886
April 2015	SSPM	9.3262*Nugget+62.661*J-Bessel(25843,1.4234)
	PRF	0.549781907249476 * x + 1.19371554328239
May 2015	SSPM	9.2755*Nugget+62.584*J-Bessel(25571,1.4822)
	PRF	0.553480748468507 * x + 1.17749047282423
June 2015	SSPM	9.336*Nugget+62.81*J-Bessel(25980,1.3949)
	PRF	0.552200654579871 * x + 1.18989463480857
July 2015	SSPM	9.4146*Nugget+62.41*J-Bessel(25843,1.4234)
	PRF	0.550391387170895 * x + 1.17803888649086
August 2015	SSPM	9.4319*Nugget+62.167*J-Bessel(25706,1.4525)
	PRF	0.549502416610134 * x + 1.17896064397254
September 2015	SSPM	9.4319*Nugget+62.167*J-Bessel(25706,1.4525)
	PRF	0.549502416610134 * x + 1.17896064397254
October 2015	SSPM	9.4232*Nugget+62.073*J-Bessel(25436,1.5125)
	PRF	0.551209178749551 * x + 1.19256718827733
November 2015	SSPM	9.3938*Nugget+62.529*J-Bessel(25843,1.4234)
	PRF	0.550404392467648 * x + 1.19548014888526
December 2015	SSPM	9.039*Nugget+61.096*J-Bessel(25843,1.433)
	PRF	0.552513086957956 * x + 1.18670932287483
January 2016	SSPM	9.8914*Nugget+75.072*J-Bessel(24844,1.2864)
	PRF	0.542306516083507 * x + 1.4958392412262
February 2016	SSPM	9.8557*Nugget+72.762*J-Bessel(24568,1.3577)
	PRF	0.532760750576408 * x + 1.49964950015477
March 2016	SSPM	9.3634*Nugget+78.103*J-Bessel(25548,1.3039)
	PRF	0.545485532037784 * x + 1.51545684348124
April 2016	SSPM	9.7713*Nugget+64.612*J-Bessel(21727,1.6849)
	PRF	0.544024854508689 * x + 1.44969237065449
May 2016	SSPM	9.519*Nugget+77.62*J-Bessel(25405,1.3305)
	PRF	0.542212194265383 * x + 1.50137847925103
June 2016	SSPM	9.9482*Nugget+69.591*J-Bessel(23626,1.3949)
	PRF	0.536184134198636 * x + 1.48423312898896
July 2016	SSPM	9.9463*Nugget+69.561*J-Bessel(23494,1.4234)
	PRF	0.538166412931703 * x + 1.47937043930584
August 2016	SSPM	9.9561*Nugget+72.849*J-Bessel(24295,1.4138)
	PRF	0.530790183980625 * x + 1.49426289215953
September 2016	SSPM	9.8249*Nugget+77.107*J-Bessel(25548,1.2864)
	PRF	0.530402716930797 * x + 1.51485235728876
October 2016	SSPM	9.9192*Nugget+73.852*J-Bessel(24844,1.2951)
	PRF	0.531615422320182 * x + 1.50916070078153
November 2016	SSPM	10.066*Nugget+72.458*J-Bessel(24295,1.4138)
	PRF	0.528628179791613 * x + 1.50623662109016
December 2016	SSPM	9.6822*Nugget+77.073*J-Bessel(25548,1.3039)
	PRF	0.531289375607921 * x + 1.50599017554534
January 2017	SSPM	9.5768*Nugget+77.699*J-Bessel(25835,1.2271)
	PRF	0.546091243785124 * x + 1.53103281010088
February 2017	SSPM	9.5655*Nugget+77.347*J-Bessel(25264,1.3486)
	PRF	0.54614794444855 * x + 1.51138151584349
March 2017	SSPM	9.9752*Nugget+66.132*J-Bessel(22343,1.5023)
	PRF	0.548614406792208 * x + 1.50673566587642
April 2017	SSPM	9.9752*Nugget+66.132*J-Bessel(22343,1.5023)
	PRF	0.548614406792208 * x + 1.50673566587642
May 2017	SSPM	10.279*Nugget+57.126*J-Bessel(20205,1.629)
	PRF	0.551285010296317 * x + 1.46938426984282
June 2017	SSPM	9.8673*Nugget+66.186*J-Bessel(22094,1.5749)
	PRF	0.551324155213397 * x + 1.46790008990546
July 2017	SSPM	9.8486*Nugget+66.444*J-Bessel(22218,1.5434)
	PRF	0.551393994087057 * x + 1.46943069576528

SSPM: Statistical Spatial Prediction Model, PRF: Predicted Regression function

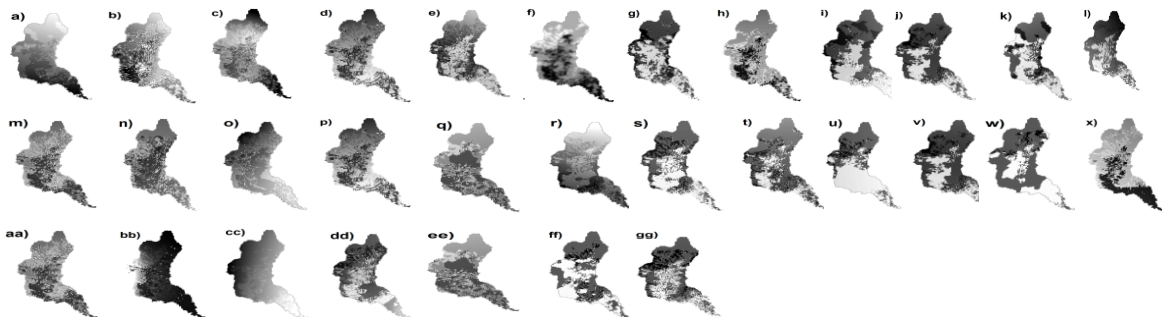


	a	b	c	d	e	f	g	h	i	j	k	l
Min.	1	3	0	20	25	33	33	36	21	30	26	15
Máx.	5	9	4	34	46	79	67	79	67	61	51	21

	m	n	o	p	q	r	s	t	u	v	w	x
Min.	0	0	0	0	31	33	33	34	30	30	34	15
Máx.	1	1	3	4	60	68	68	76	60	60	75	20

	y	z	aa	bb	cc	dd	ee
Min.	33	0	11	33	113	34	34
Máx.	69	11	15	69	126	74	79

Fig: 11. Spatial prediction of the monthly infiltration (mm) that occurred over the aquifer of San Diego Municipality during the period 2015-2017: Figure 11a - l: January-December 2015, Figure 11m-x: January-December 2016, Figure 11y-e: January - July 2017.



	a	b	c	d	e	f	g	h	i	j	k	l
Min.	-14	-	-19	-	-	-12	-12	-96	-12	-12	-13	-13
Máx.	-13	-	-17	-	-	-10	-10	-46	-6	-8	-10	-10
		21		16	17							
		19		14	14							

	m	n	o	p	q	r	s	t	u	v	w	x
Min.	-18	-17	-24	-24	-	-12	-6	-92	-8	-6	21	-9
Máx.	-17	-16	-21	-21	31	0	-1	-52	-3	-1	26	-8

	y	z	aa	bb	cc	dd	ee
Min.	-31	-	-13	-10	-	-10	-10
		48			10		
Máx.	40	-9	-	-5	-5	-5	-8
			11				

Fig: 12. Spatial prediction of the monthly volume stored (mm) that occurred over the aquifer of San Diego Municipality during the period 2015-2017: Figure 12a - l: January-December 2015, Figure 12m-x: January-December 2016, Figure 12y-e: January - July 2017.

Table: 6. Results of the application of the ordinary kriging space prediction model of the monthly infiltration (mm/month) on the aquifer of San Diego Municipality, Carabobo State.

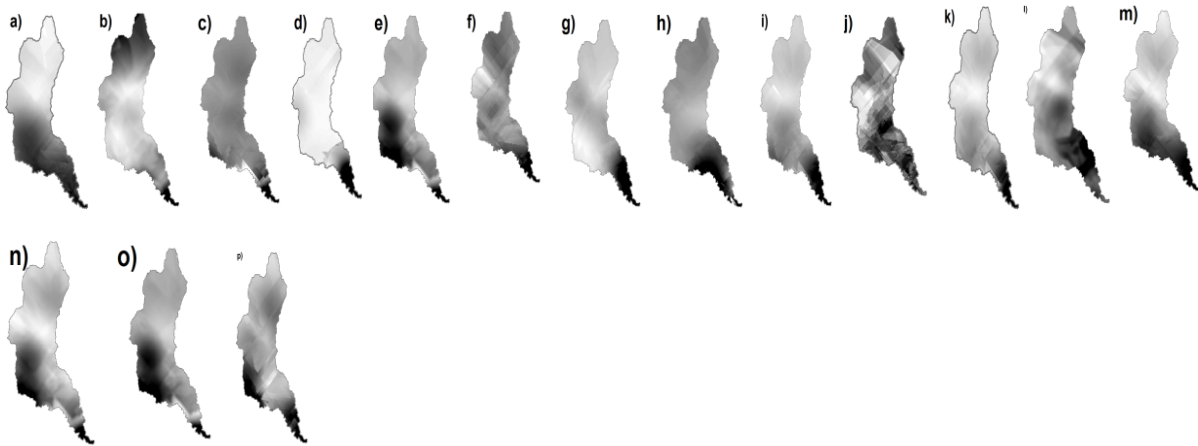
Month	SSPM	Ordinary Krigging
January 2015	SSPM	0.19657*Nugget+0.46952*J-Bessel(6035.6,3.9154)
	PRF	0.914190896029479 * x + 0.253452895027796
February 2015	SSPM	0.67583*Nugget+0.96255*J-Bessel(4674.3,3.3077)
	PRF	0.762089612759152 * x + 1.38319018235861
March 2015	SSPM	0.38596*Nugget+0.11568*J-Bessel(5024.3,10)
	PRF	0.544345605828489 * x + 0.639435525022578
April 2015	SSPM	10.525*Nugget+6.0109*J-Bessel(10781.4,3323)
	PRF	0.659079012190774 * x + 8.73857908427838
May 2015	SSPM	24.943*Nugget+17.633*J-Bessel(2230.2,4.5418)
	PRF	0.585765195061831 * x + 14.6805940045912
June 2015	SSPM	105.67*Nugget+71.5*J-Bessel(2821.2,5.7902)
	PRF	0.619465615509927 * x + 22.3189568030305
July 2015	SSPM	63.571*Nugget+50.776*J-Bessel(3760.1,5.0937)
	PRF	0.694848180252544 * x + 14.9847075790972
August 2015	SSPM	118.53*Nugget+86.797*J-Bessel(10781.6,8539)
	PRF	0.745364051940763 * x + 15.8793762762709
September 2015	SSPM	98.435*Nugget+81.538*J-Bessel(7907.6,10)
	PRF	0.770641976651541 * x + 13.5589515649548
October 2015	SSPM	35.712*Nugget+44.64*J-Bessel(4204.7,1.1705)
	PRF	0.75753021951756 * x + 11.9132985428515
November 2015	SSPM	31.3*Nugget+34.363*J-Bessel(4609.2,10)
	PRF	0.789772056113103 * x + 8.16059018119337
December 2015	SSPM	1.1119*Nugget+0.98826*J-Bessel(1732.6,4.7294)
	PRF	0.585803464433969 * x + 7.58240428229607
January 2016	SSPM	0*Nugget+0.00037546*J-Bessel(143.68,7.2339)
	PRF	0.998340562984084 * x + 0.000522546279174085
February 2016	SSPM	0.0093793*Nugget+0.0020918*J-Bessel(194.03,0.1298)
	PRF	0.984383003011847 * x + -0.00285817843860336
March 2016	SSPM	0.081671*Nugget+0.388*J-Bessel(10761.3,6847)
	PRF	0.969167042820265 * x + 0.00199153928813317
April 2016	SSPM	0*Nugget+197.53*J-Bessel(10684.2,0767)
	PRF	0.997294604926262 * x + 0.38027154954699
May 2016	SSPM	69.507*Nugget+53.299*J-Bessel(1923.4,5.7126)
	PRF	0.640999917062122 * x + 16.7204195976351
June 2016	SSPM	71.852*Nugget+72.175*J-Bessel(4302.5,10)
	PRF	0.681839724061845 * x + 15.9604874268722
July 2016	SSPM	58.252*Nugget+64.196*J-Bessel(2998.4,4.4508)
	PRF	0.712646362692372 * x + 14.3430878942266
August 2016	SSPM	66.651*Nugget+51.651*J-Bessel(3503.5,10)
	PRF	0.558059828529455 * x + 23.4566811308446
September 2016	SSPM	57.882*Nugget+116.89*J-Bessel(7223.6,3.0712)
	PRF	0.880727293021719 * x + 5.83936601008649
October 2016	SSPM	36.747*Nugget+29.651*J-Bessel(1481.3,4.0771)
	PRF	0.562940212494382 * x + 21.1948725316548
November 2016	SSPM	43.752*Nugget+98.372*J-Bessel(3131.8,4.3616)
	PRF	0.854140784839132 * x + 7.94536950053569
December 2016	SSPM	0.60423*Nugget+0.90813*J-Bessel(1759.5,4.1605)
	PRF	0.783456526648032 * x + 3.91013289824423
January 2017	SSPM	74.714*Nugget+78.735*J-Bessel(3663.1,4.7614)
	PRF	0.763988616775912 * x + 12.4957775000195
February 2017	SSPM	0.13892*Nugget+4.7406*J-Bessel(6668.1,2.3449)
	PRF	0.991196314259762 * x + 0.0147464002316315
March 2017	SSPM	0.17684*Nugget+0.28616*J-Bessel(10781.3,1765)
	PRF	0.765303364414884 * x + 2.91375268387473
April 2017	SSPM	103.3*Nugget+56.006*J-Bessel(4896.8,10)
	PRF	0.583154841945897 * x + 22.153330573496
May 2017	SSPM	0.079855*Nugget+4.0457*J-Bessel(6915.9,2.3767)
	PRF	0.98481614259524 * x + 1.80465177974914
June 2017	SSPM	80.288*Nugget+102.21*J-Bessel(2946.7,4.7936)
	PRF	0.73550053866666 * x + 14.0729933066227
July 2017	SSPM	89.015*Nugget+63.751*J-Bessel(3214.7,4.5112)
	PRF	0.563641606933269 * x + 24.9208079034558

SSPM: Statistical Spatial Prediction Model, PRF: Predicted Regression function

Table: 7. Results of the application of the ordinary krigging space prediction model of the monthly volume stored (mm/month) in the aquifer of San Diego Municipality, Carabobo State.

Volume stored in aquifer	SSPM	Ordinary Krigging
January 2015	SSPM	0.041056*Nugget+3.2377*J-Bessel(10625,2.4253)
	PRF	0.993552816661224 * x + -0.750641419388359
February 2015	SSPM	0.026382*Nugget+1.4877*J-Bessel(5085.1,2.8324)
	PRF	0.988024466461108 * x + -2.00027558421908
March 2015	SSPM	0.09486*Nugget+0.61309*J-Bessel(10393,3.5148)
	PRF	0.970700418662774 * x + -4.44967185158484
April 2015	SSPM	1.3163*Nugget+4.9763*J-Bessel(3985.8,6.9003)
	PRF	0.949568599135324 * x + -6.68087583116392
May 2015	SSPM	1.2286*Nugget+15.824*J-Bessel(2284.2,5.8689)
	PRF	0.953110919779727 * x + -6.14271947584258
June 2015	SSPM	8.4411*Nugget+67.306*J-Bessel(2671.4,7.9504)
	PRF	0.962020661664087 * x + -2.58595346440146
July 2015	SSPM	21.787*Nugget+50.749*J-Bessel(5909.5,10)
	PRF	0.945160360976187 * x + -4.41891030483822
August 2015	SSPM	18.234*Nugget+76.713*J-Bessel(4363.3,10)
	PRF	0.954803313637495 * x + -3.63145184228314
September 2015	SSPM	2.3296*Nugget+64.085*J-Bessel(3653.8,5.8689)
	PRF	0.986850520970233 * x + -0.901183257315651
October 2015	SSPM	5.8315*Nugget+48.236*J-Bessel(4039.7,10)
	PRF	0.965162376033881 * x + -2.91520876926374
November 2015	SSPM	0.7682*Nugget+31.272*J-Bessel(2152.5,5.9086)
	PRF	0.976624249596379 * x + -2.37810700126352
December 2015	SSPM	1.7909*Nugget+2.6196*J-Bessel(10781,3.5386)
	PRF	0.786060703544889 * x + -20.0498633992544
January 2016	SSPM	0.00010747*Nugget+0.0033732*J-Bessel(3295.2,2.6476)
	PRF	0.994398326672517 * x + -0.790366381117337
February 2016	SSPM	0*Nugget+0.10606*J-Bessel(10709,2.1772)
	PRF	0.997756201797346 * x + -0.308619005881496
March 2016	SSPM	90.44*Nugget+72.897*J-Bessel(2803.4,7.2339)
	PRF	0.669646171224709 * x + 16.7464300411453
April 2016	SSPM	28.724*Nugget+82.37*J-Bessel(5820.1,10)
	PRF	0.951337738214618 * x + -4.29620083527587
May 2016	SSPM	3.4619*Nugget+49.494*J-Bessel(1954.9,8.7379)
	PRF	0.947561154050223 * x + -3.82353634541636
June 2016	SSPM	13.141*Nugget+72.373*J-Bessel(4273.1,10)
	PRF	0.957942906872725 * x + -2.87766112223862
July 2016	SSPM	12.484*Nugget+66.14*J-Bessel(4328.2,10)
	PRF	0.956887885868877 * x + -4.04333542667264
August 2016	SSPM	54.736*Nugget+45.059*J-Bessel(1547.2,4.1047)
	PRF	0.558117809950964 * x + -30.7730924590625
September 2016	SSPM	9.6115*Nugget+133.14*J-Bessel(7720.4,10)
	PRF	0.984052363513413 * x + -0.821785068752504
October 2016	SSPM	14.304*Nugget+115.72*J-Bessel(7264.3,4.8916)
	PRF	0.982975845996658 * x + -1.26666669703083
November 2016	SSPM	15.071*Nugget+96.349*J-Bessel(4632.2,10)
	PRF	0.974591562997573 * x + -0.799680854587752
December 2016	SSPM	0.17135*Nugget+1.0259*J-Bessel(4374.9,10)
	PRF	0.973952834084664 * x + -1.87945028218256
January 2017	SSPM	95.717*Nugget+212.43*J-Bessel(10781,3.5386)
	PRF	0.877752221734397 * x + 1.23544591597926
February 2017	SSPM	0.01916*Nugget+2.3556*J-Bessel(10741,2.3607)
	PRF	0.995658648693613 * x + -0.344724668651608
March 2017	SSPM	0*Nugget+12.222*J-Bessel(10745,2.1192)
	PRF	1.0000118105764 * x + 0.000914147703568347
April 2017	SSPM	0*Nugget+3.4151*J-Bessel(5547.3,2.3449)
	PRF	0.999953461566654 * x + -0.00363462687616334
May 2017	SSPM	0*Nugget+4.445*J-Bessel(6157.7,2.2067)
	PRF	0.999861936140516 * x + 0.00087234685464832
June 2017	SSPM	8.8374*Nugget+93.683*J-Bessel(2839.1,7.3818)
	PRF	0.959384954503971 * x + -2.80136450280715
July 2017	SSPM	34.599*Nugget+108.63*J-Bessel(10745,6.762)
	PRF	0.968084885842449 * x + -2.27369559501686

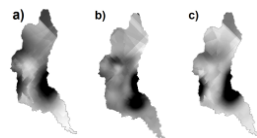
SSPM: Statistical Spatial Prediction Model, PRF: Predicted Regression function



	a	b	c	d	e	f	g	h	i	j	k	l
Min.	81	5	0	0	0	6	0	0	87	27	188	6
Máx.	333	81	461	18	123	45	219	17	1384	28	2341	8

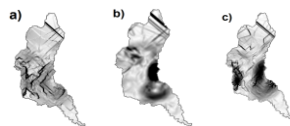
	m	n	o	p
Min.	91	52	0	22
Máx.	318	618	295	232

Fig: 13. Spatial prediction of the physico-chemical parameters that occurred over the aquifer of San Diego Municipality during the period 2015-2017: a) Bicarbonate (mg/l) b) Chloride (mg/l), c) Sulfate (mg/l), d) Nitrate (mg/l), e) Calcium (mg/l), f) Magnesium (mg/l), g) Sodium (mg/l), h) Potassium (mg/l), i) Dissolved Solids (mg/l), j) Temperature (°C), k) Electrical conductivity ($\mu\text{S}/\text{cm}$), l) pH, m) Alkalinity (mg/l CaCO_3), n) Total Hardness (mg/l CaCO_3), o) Calcic hardness (mg/l CaCO_3), p) Magnesium hardness (mg/l CaCO_3).



	a	b	c
Min.	385	329	364
Máx.	574	803	787

Fig: 14. Spatial prediction of the Dynamic Level expressed in meter above sea level (masl) that occurred over the aquifer of San Diego Municipality during the period 2015-2017: a) Dynamic Level for 2015, b) Dynamic Level for 2016, c) Dynamic Level for 2017.



	a	b	c
Min.	0	0	0
Máx.	39	29	55

Fig: 15. Spatial prediction of the Hydraulic Gradient expressed in percentage that occurred over the aquifer of San Diego Municipality during the period 2015-2017: a) Dynamic Level for 2015, b) Dynamic Level for 2016, c) Dynamic Level for 2017.

Table: 8. Results of the application of the ordinary krigging space prediction model of the monthly Physico-Chemical Parameters in the period 2015-2018 in the aquifer of San Diego Municipality, Carabobo State.

Physico-Chemical Parameters	Unit	SSPM	Ordinary Krigging
Bicarbonate	mg/l	SSPM	6617*Nugget+3660.3*J-Bessel(9786.1,5.1282)
		PRF	0.425827322519084 * x + 81.2268753366656
Chloride	mg/l	SSPM	264.95*Nugget+483.32*J-Bessel(9386,6.947)
		PRF	0.486048978022043 * x + 5.49184970765876
Sulfate	mg/l	SSPM	6738.9*Nugget+25336*J-Bessel(9771,10)
		PRF	0.349967778608995 * x + 14.8980871444998
Nitrate	mg/l	SSPM	12.952*Nugget+14.159*Stable(5492,9.2)
		PRF	0.0122495930970624 * x + 0.27473123657915
Calcium	mg/l	SSPM	634.52*Nugget+1740.6*J-Bessel(10349,7.089)
		PRF	0.367722826720686 * x + 16.1406609252905
Magnesium	mg/l	SSPM	229.49*Nugget+318.88*J-Bessel(21347,0.91193)
		PRF	0.314111548128062 * x + 6.7453870344574
Sodium	mg/l	SSPM	828.52*Nugget+1593.5*J-Bessel(9129,3.134)
		PRF	0.569176969134538 * x + 9.72058527320901
Potassium	mg/l	SSPM	50.336*Nugget+96.802*J-Bessel(11719,10)
		PRF	0.125352671552489 * x + 1.9716072738805
Silica	mg/l	SSPM	140.82*Nugget+328.96*J-Bessel(4679.5,10)
		PRF	0.295522537341314 * x + 22.325936878676
DissolvedSolids	mg/l	SSPM	45756*Nugget+104210*J-Bessel(9492.7,4.3323)
		PRF	0.481170950272245 * x + 109.913217854712
Temperature	°C	SSPM	1.0368*Nugget+1.1653*J-Bessel(42219,1.7903)
		PRF	0.280641432307401 * x + 19.3332817803927
Electric conductivity	µS/cm	SSPM	82890*Nugget+221200*J-Bessel(9839.3,4.8261)
		PRF	0.54105814683103 * x + 138.314187003829
Ph	-	SSPM	0.37515*Nugget+0.44952*J-Bessel(10650,1.6963)
		PRF	0.229237983403226 * x + 5.49145154485519
Alkalinity	mg/l CaCO ₃	SSPM	4349.1*Nugget+4949.9*J-Bessel(22035,0.11652)
		PRF	0.457614421912662 * x + 66.6682678330272
Total hardness	mg/l CaCO ₃	SSPM	13705*Nugget+37920*J-Bessel(10028,7.5837)
		PRF	0.437956501549915 * x + 57.5655670814896
Calcichardness	mg/l CaCO ₃	SSPM	4048.2*Nugget+10976*J-Bessel(9989.5,7.3322)
		PRF	0.376751448457521 * x + 40.2905328839105
Magnesiumhardness	mg/l CaCO ₃	SSPM	8730.2*Nugget+10342*J-Bessel(10587,8.2232)
		PRF	0.272421185584737 * x + 36.4172496252133

Table: 9. Results of the application of the ordinary krigging space prediction model of the monthly dynamic level in the period 2015-2017 in the aquifer of San Diego Municipality, Carabobo State.

Dynamic Level (masl)	SSPM	Ordinary Krigging
2015	SSPM	1281.6*Nugget+5000.7*J-Bessel(14136,10)
	PRF	0.886789498938431 * x + 55.0733317327875
2016	SSPM	821.68*Nugget+4282.7*J-Bessel(12219,10)
	PRF	0.89821359094478 * x + 48.1367583450571
2017	SSPM	176.81*Nugget+4675.5*J-Bessel(7560.2,10)
	PRF	0.969348388121472 * x + 13.9818799467086

Table: 10. Results of the application of the ordinary krigging space prediction model of the monthly hydraulic gradient in the period 2015-2017 in the aquifer of San Diego Municipality, Carabobo State.

Dynamic Level (masl)	SSPM	Ordinary Krigging
2015	SSPM	$2.0954 * \text{Nugget} + 6.1085 * \text{J-Bessel}(795.48, 10)$
	PRF	$0.779008025304863 * x + 0.592618823186321$
2016	SSPM	$3.7767 * \text{Nugget} + 15.52 * \text{J-Bessel}(3227, 5.7513)$
	PRF	$0.976192672636932 * x + 0.0976006080717546$
2017	SSPM	$24.011 * \text{Nugget} + 16.047 * \text{J-Bessel}(12496, 0.039596)$
	PRF	$0.842709213319876 * x + 0.875085452933433$

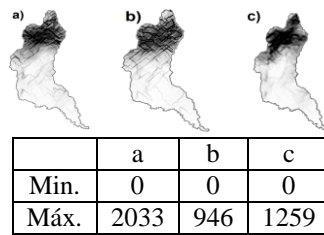


Fig: 16. Spatial prediction of the Flow Velocity expressed in m/d that occurred over the aquifer of San Diego Municipality during the period 2015-2017: a) Flow Velocity for 2015, b) Flow Velocity for 2016, c) Flow Velocity for 2017.

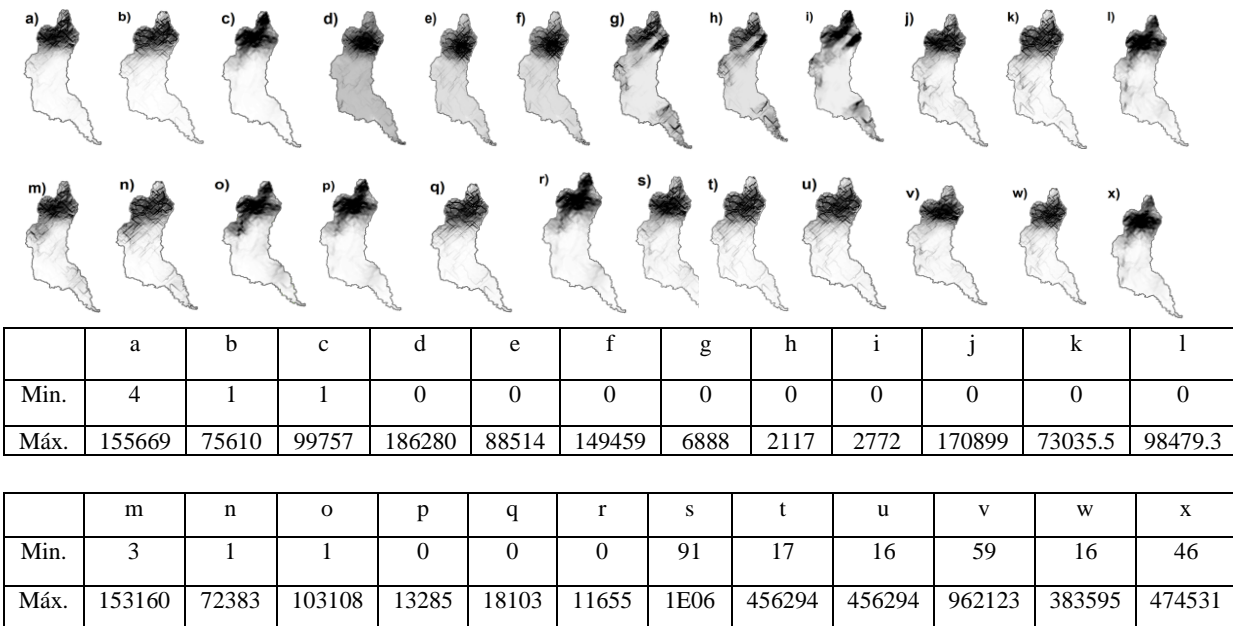


Fig: 17. Spatial prediction of the mass flow of physico-chemical parameters that occurred over the aquifer of San Diego Municipality during the period 2015-2017: a) Chloride for 2015 (kg/d), b) Chloride for 2016 (kg/d), c) Chloride for 2017 (kg/d), d) Sulfate for 2015(kg/d), e) Sulfate for 2016 (kg/d), f) Sulfate for 2017 (kg/d), g) Nitrite for 2015 (kg/d), h) Nitrite for 2016 (kg/d), i) Nitrite for 2017 (kg/d), j) Calcium for 2015 (kg/d), k) Calcium for 2016 (kg/d), l) Calcium for 2017 (kg/d), m) Sodium for 2015 (kg/d), n) Sodium for 2016 (kg/d), o) Sodium for 2017 (kg/d), p) Potassium for 2015 (kg/d), q) Potassium for 2016 (kg/d), r) Potassium for 2017 (kg/d), s) Alkalinity for 2015 (kg/d), t) Alkalinity for 2016 (kg/d), u) Alkalinity for 2017 (kg/d), v) Total Hardness for 2015 (kg/d), w) Total Hardness for 2016 (kg/d), x) Total Hardness for 2017 (kg/d).

Water Classification

The water classification of the San Diego aquifer based on the Piper-Hill-Langelier diagram using the physico-chemical parameters measured in the aquifer during the period 2015-2017 is shown in Figure 18. Four water classes are found in the aquifer, which are the following: 1) Bicarbonate of Calcium and/or Magnesium, 2) Bicarbonate of Sodium, 3) Sulfate or Chloride of Calcium and/or Magnesium, 4) Sulfate and/or Chloride of Sodium. These water classes have been located in the aquifer regions as follows: 1) North and Middle: the water predominantly contains bicarbonate of calcium and/or magnesium in an area of 95.17 km², 2) Middle and South: the water contains bicarbonate of sodium in an area of 19.32 km², 3) South: the water contains two constituents: sulfate of sodium in an area of 0.96 km² and sulfate of magnesium and/or calcium in an area of 1.68 km². The equation is identified by the following coefficients in a general structure: $a \cdot \text{nugget} + b(J\text{-Bessel}(c, d))$. The values of coefficients vary according to the neighbors values in each dataset of water classification are as follows (Table 12): a: 0.027285, b: 0.14414, c: 10781, d: 2.7384.

DISCUSSION

Geophysical parameters

With respect the geophysical parameters, the effective porosity varies according to the unconsolidated sediments as follows (Matthess and Ubell, 2003): 1) silt: between 0 and 12% corresponding to mean grain diameter between 0.001 and 0.01 mm, 2) sand: between 12 and 40 % corresponding to mean grain diameter between 0.01 and 1.0 mm, 3) gravel: between 40 and 42 % corresponding to mean grain diameter between 1 and 10 mm. The San Diego aquifer includes alternating layers of soil material predominantly between well-graded sand and clay of low plasticity, being confined aquifer. The gravel is the unique aquifer material in the three profiles close to the mountain zone identified as: PW5, PW19 and PW27 where the recharge zones might be located (Figure 2, Figure 3, Table 1). The permeability or hydraulic conductivity varies with respect the effective porosity as follows (Marotz, 1968): 1) silt: between 0 and 12% corresponding to permeability between 10^{-4} and 10^{-3} m/s (from 8.64 to 86.4 m/d), 2) sand: between 12 and 40 % corresponding to permeability between 10^{-3} and 10^{-2} m/s (from 86.4 to 864 m/d) to , 3) gravel (Figure 4): between 40 and 42 % corresponding to permeability upper 10^{-2} m/s (> 864 m/d). The San Diego aquifer has a permeability varying from 100 to 1000 m/d, the trend is close to 100 m/d.



Fig: 18. Spatial prediction of the water classification based on Piper-Hill-Langeley diagram from physico-chemical parameters that occurred over the aquifer of San Diego Municipality during the period 2015-2017: 1) Bicarbonate of Calcium and/or Magnesium, 2) Bicarbonate of Sodium, 3) Sulfate or Chloride of Calcium and/or Magnesium, 4) Sulfate and/or Chloride of Sodium.

Table: 11. Results of the application of the ordinary krigging space prediction model of the monthly mass flow of constituents in the period 2015-2017 in the aquifer of San Diego Municipality, Carabobo State.

Physico-Chemical Parameters	Unit	SSPM	Ordinary Krigging
Chloride	2015	kg/d	SSPM 2.7582e7*Nugget+3.0076e7*J-Bessel(612.15,10) PRF 0.970690931345482 * x + 259.192635711595
		kg/d	SSPM 5768300*Nugget+2.2261e7*J-Bessel(307.93,1.64) PRF 0.932617217315471 * x + 220.549027200017
	2016	kg/d	SSPM 5.4886e7*Nugget+8.609e8*J-Bessel(25720,3.8891) PRF 0.99183140652004 * x + 50.8787834846989
		kg/d	SSPM 9.4394e7*Nugget+4.0232e8*J-Bessel(17171,10) PRF 0.967680617047796 * x + 347.182270055646
	2017	kg/d	SSPM 4.0905e7*Nugget+1.9622e8*J-Bessel(17183,9.866) PRF 0.892678880928101 * x + 594.383967807894
		kg/d	SSPM 86107*Nugget+174540*J-Bessel(22001,0.01) PRF 0.923387631591934 * x + 20.0989303819858
Sulfate	2015	kg/d	SSPM 29152*Nugget+73549*J-Bessel(22053,0.01) PRF 0.809999637134594 * x + 28.4474817066939
		kg/d	SSPM 14804*Nugget+86384*J-Bessel(3286.8,10) PRF 0.984961006977312 * x + 3.84440804336509
	2016	kg/d	SSPM 2.4252e7*Nugget+4.2065e7*J-Bessel(714.39,10) PRF 0.963078986607316 * x + 442.425606849161
		kg/d	SSPM 2.2757e7*Nugget+1.3405e7*J-Bessel(1130.2,10) PRF 0.877518240681205 * x + 736.330752917085
	2017	kg/d	SSPM 6.8854e7*Nugget+6.3276e8*J-Bessel(25717,8.4481) PRF 0.990036693326733 * x + 89.1459920155085
		kg/d	SSPM 3.012e7*Nugget+3.5688e7*J-Bessel(640.28,10) PRF 0.961534926414707 * x + 510.47664313321
Nitrate	2015	kg/d	SSPM 1.9998e7*Nugget+1.874e7*J-Bessel(678.67,10) PRF 0.8865410509426 * x + 715.621954863157
		kg/d	SSPM 8.0612e7*Nugget+7.5696e8*J-Bessel(25720,4.6035) PRF 0.990014885086545 * x + 101.015426514978
	2016	kg/d	SSPM 1307800*Nugget+1.6216e7*J-Bessel(25720,4.666) PRF 0.991118774632633 * x + 10.4367655743274
		kg/d	SSPM 548730*Nugget+217370*J-Bessel(1484.8,10) PRF 0.885849471680117 * x + 93.410040451226
	2017	kg/d	SSPM 1307800*Nugget+1.6216e7*J-Bessel(25720,4.666) PRF 0.991118774632633 * x + 10.4367655743274
		kg/d	SSPM 9.6802e8*Nugget+1.3745e9*J-Bessel(569.2,10) PRF 0.968612737458134 * x + 2466.5208930974
Calcium	2015	kg/d	SSPM 1.3508e9*Nugget+7.2914e9*J-Bessel(22264,0.01) PRF 0.883987346847367 * x + 4529.45395386129
		kg/d	SSPM 1.3508e9*Nugget+7.2914e9*J-Bessel(22264,0.01) PRF 0.883987348817566 * x + 4529.4538884111
	2016	kg/d	SSPM 6.2119e8*Nugget+9.7618e8*J-Bessel(539.3,10) PRF 0.96995138734539 * x + 1901.07717660229
		kg/d	SSPM 9.7562e8*Nugget+4.6656e9*J-Bessel(20405,0.01) PRF 0.886670763670727 * x + 3551.48127009171
	2017	kg/d	SSPM 1.9452e9*Nugget+1.8055e10*J-Bessel(24494,10) PRF 0.991113718713541 * x + 416.62067036287
		kg/d	SSPM 0.991113718713541 * x + 416.62067036287
Sodium	2015	kg/d	SSPM 6.2119e8*Nugget+9.7618e8*J-Bessel(539.3,10) PRF 0.96995138734539 * x + 1901.07717660229
		kg/d	SSPM 9.7562e8*Nugget+4.6656e9*J-Bessel(20405,0.01) PRF 0.886670763670727 * x + 3551.48127009171
	2016	kg/d	SSPM 1.9452e9*Nugget+1.8055e10*J-Bessel(24494,10) PRF 0.991113718713541 * x + 416.62067036287
		kg/d	SSPM 0.991113718713541 * x + 416.62067036287
	2017	kg/d	SSPM 6.2119e8*Nugget+9.7618e8*J-Bessel(539.3,10) PRF 0.96995138734539 * x + 1901.07717660229
		kg/d	SSPM 9.7562e8*Nugget+4.6656e9*J-Bessel(20405,0.01) PRF 0.886670763670727 * x + 3551.48127009171
Potassium	2015	kg/d	SSPM 1.9452e9*Nugget+1.8055e10*J-Bessel(24494,10) PRF 0.991113718713541 * x + 416.62067036287
		kg/d	SSPM 0.991113718713541 * x + 416.62067036287
	2016	kg/d	SSPM 6.2119e8*Nugget+9.7618e8*J-Bessel(539.3,10) PRF 0.96995138734539 * x + 1901.07717660229
		kg/d	SSPM 9.7562e8*Nugget+4.6656e9*J-Bessel(20405,0.01) PRF 0.886670763670727 * x + 3551.48127009171
	2017	kg/d	SSPM 1.9452e9*Nugget+1.8055e10*J-Bessel(24494,10) PRF 0.991113718713541 * x + 416.62067036287
		kg/d	SSPM 0.991113718713541 * x + 416.62067036287
Alkalinity (CaCO₃)	2015	kg/d	SSPM 6.2119e8*Nugget+9.7618e8*J-Bessel(539.3,10) PRF 0.96995138734539 * x + 1901.07717660229
		kg/d	SSPM 9.7562e8*Nugget+4.6656e9*J-Bessel(20405,0.01) PRF 0.886670763670727 * x + 3551.48127009171
	2016	kg/d	SSPM 1.9452e9*Nugget+1.8055e10*J-Bessel(24494,10) PRF 0.991113718713541 * x + 416.62067036287
		kg/d	SSPM 0.991113718713541 * x + 416.62067036287
	2017	kg/d	SSPM 6.2119e8*Nugget+9.7618e8*J-Bessel(539.3,10) PRF 0.96995138734539 * x + 1901.07717660229
		kg/d	SSPM 9.7562e8*Nugget+4.6656e9*J-Bessel(20405,0.01) PRF 0.886670763670727 * x + 3551.48127009171
Total hardness (CaCO₃)	2015	kg/d	SSPM 1.9452e9*Nugget+1.8055e10*J-Bessel(24494,10) PRF 0.991113718713541 * x + 416.62067036287
		kg/d	SSPM 0.991113718713541 * x + 416.62067036287
	2016	kg/d	SSPM 6.2119e8*Nugget+9.7618e8*J-Bessel(539.3,10) PRF 0.96995138734539 * x + 1901.07717660229
		kg/d	SSPM 9.7562e8*Nugget+4.6656e9*J-Bessel(20405,0.01) PRF 0.886670763670727 * x + 3551.48127009171
	2017	kg/d	SSPM 1.9452e9*Nugget+1.8055e10*J-Bessel(24494,10) PRF 0.991113718713541 * x + 416.62067036287
		kg/d	SSPM 0.991113718713541 * x + 416.62067036287

Table: 12. Results of the application of the ordinary krigging space prediction model of the water classification in terms of the constituents according to the Piper-Hill-Langelier diagram during the period 2015-2017 in the aquifer of San Diego Municipality, Carabobo State.

Physico-Chemical Parameters		SSPM	Ordinary Krigging
WaterClassification	2015-2017	SSPM PRF	$0.027285 * \text{Nugget} + 0.14414 * \text{J-Bessel}(10781, 2.7384)$ $0.99999999999892 * x + 4.18687307046639e-12$

Land Use / Land Cover

Most of the wells are located in the north and middle regions of the aquifer, where 20 wells are used for human consumption in residential zones. The rest of the wells located in the south region, being used for industrial and agricultural activities (Figure 5). According to Bear and Cheng (2010), an aquifer is used as: source of water, storage reservoir, conduit and filter plant. The San Diego aquifer is a source of water and storage reservoir; being a renewable resource because of the precipitation; which depends on the distribution of storms, land topography and cover, permeability of soil, infiltrates through the ground surface and replenishes the underlying phreatic aquifer. Hydrological processes in the San Diego aquifer such as infiltration and permeability are influenced by the impermeability in the urban area of the Sand Diego aquifer, which is around 20% of the total area, reducing the contribution rates to the aquifer water. The San Diego aquifer is not used as a conduit and filtration plant; implying the application of artificial recharge techniques, because in Venezuela it is prohibited by water regulation. The land use and land cover in the San Diego aquifer expressed by the mean and standard deviation of the area varies during the period 2015-2017 as follows: urban: 34, 8 km², agricultural: 7, 7 km², vegetation: 49, 15 km², degraded soil: 26, 11 km². By comparing, Marquez et al., (2018) analyze results depicted by the area change detection methods in the Pao river basin based on post-classification using Maximum Likelihood (ML) during

the period 1986 – 2018 expressed by the area change detection percentage according each class finding the following results: a) U: Urban: 18 to 40% b) A: Agricultural: 85 to 95% c) R: Rangeland: 80 to 95%, d) W: Water: 10 to 20% e) V: Vegetation: 5 to 10%, f) D.S.: Degraded Soil: 55 to 60%. In the period analyzed the urban and agricultural classes shows a slight variation compared with the vegetation and degraded soil and the changes found in the pao river basin.

Groundwater Balance

1) *Precipitation:* the annual seasons in Venezuela are divided in two periods: dry and rainy. The first comprises between November and April of each year, and the second between May and October of each year (Ramirez, 1971; Guevara and Cartaya, 2004). Ramirez, (1971) develops a procedure to determine spatial and time variations of precipitation in Venezuela based on 126 stations of measurements, finding that the precipitation in the Aragua de Barcelona station located in latitude of 9.28 °N and longitude of 64.5° W, in April, is 5 mm for the 50 percentile value and 23 mm for the mean value for month, while in June, is 148 mm for the 50 percentile value and 151 mm for the mean value for month. In general, this indicates that for the larger precipitation amounts that occur in June the variation is much less than for the dry season months such as April. By comparing with San Diego aquifer, it can be found that the variation of the precipitation is few significant between the north, central and south region during dry season regarding to the

variation occurred during the rainy season. These results are in contrast with the variation analysis reported by Ramirez, (1971) for the precipitation station used as a sample.

2) *Evapotranspiration*: according with Trezza, (2006), the evapotranspiration measured for water management in an irrigation system in Venezuela uses as a reference the meteorological station identified as “Biologica Los Llanos”, estimating the monthly mean evapotranspiration (ET) in the period 1968-2002. The ET varies between 5.0 and 7.6 mm/d (150-228 mm/month) for the dry season, and 4.5 and 5.5 mm/d (135-165 mm/month) for the rainy season, respectively. By comparing with San Diego aquifer, it can be found that the spatial variation of the evapotranspiration is insignificant between the north, central and south region during dry and rainy season. These results are lesser than those reported by Trezza, (2006) for the ET station used as a sample, being the minimum ET value estimated in San Diego aquifer the 20 % of the minimum ET observed in the “Biologica Los Llanos” station. Likewise, the maximum ET value estimated in San Diego aquifer the 80 % of the maximum ET observed in the “Biologica Los Llanos” station.

3) *Pumping flow*: the pumping flow (PF) extracted from the San Diego aquifer is estimated based on a sample of 53 wells; including domestic and industrial uses. For 2015, the PF is 129,769,378.56 m³/y. For 2016, the PF is 125,975,597.76 m³/y. For 2017, the PF is 132,612,033.60 m³/y. Pumping flow extracted has a tendency to increase over time, as the PF decreases is because pumping equipment damaged or water management company decisions of water regulating for well maintenance. By comparing with the Nile’s Delta, the groundwater abstraction by wells in the Delta has consistently increased, if judged by the number of wells inventoried (Molle et al., 2018): from 5600 wells in 1952, to

13,000 in 1991, 22,905 in 2011, and finally 32,054 agricultural wells in 2016 (Zeidan, 2016). The PF was a total of 0.2 Bm³/y in 1952, 2.77 Bm³ in 1991 and 3.5 Bm³ in 2003 (Zeidan, 2016), abstraction reached 4.9 Bm³ in 2008, according to Morsy (2009); being comparatively higher than the San Diego aquifer.

4) *Infiltration*: according to Perez and Romance, (2012) the infiltration measured in an agricultural field in Venezuela corresponding to soils of type silty sand to organic silt varies from 2 mm/h to 1200 mm/h; being the mean value of 400 mm/h. The infiltration in the San Diego aquifer is influenced by the urban zone because this can reach to 48.6% of the total area of aquifer. For that reason the infiltration takes low values. Guevara and Cartaya, (2004) indicates that the infiltration for a soil type corresponding to clay with organic matter allows the inflow to a rate in stable state of 30 to 70 mm/h as it is found in the San Diego aquifer for stable state. The infiltration in rainy season takes values higher in the vegetation and agricultural zone. Guevara and Cartaya, (2004) indicates that the infiltration for a soil type corresponding to agricultural soil with organic matter allows the inflow to a rate in stable state of 20 to 290 mm/h as it is found in the San Diego aquifer for stable state.

5) *Volume Stored*: the volume stored in the San Diego aquifer is giving negative results based on this is estimated only by three variables: 1) infiltration, which is the unique water inlet, 2) evapotranspiration and 3) pumping flow; which are water outlet. It must be considered other sources of direct recharge from the San Diego River. As it has been discuss, the San Diego aquifer is confined, the clay layers is alternating with the sand well-graded and gravel well-graded. In general, the first clay layer has a thickness that varies between 2 and 22 m creating a top, reducing the direct recharge of water (Table 1). One of the variables associated

to the direct recharge is the infiltration, which represents between 34 and 41% of the monthly precipitation. It assumes that this infiltration occurs in some parts of the aquifer where there is not the clay top as it is found in the profiles 1, 2, 5 and 12 (Table 1). As a reference, in the Guarani aquifer, The annual infiltration in 2005 was estimated to be 350 mm, while the deep recharge, based on water balance, appears to be 3.5% of the precipitation estimated in 1410 mm/y (Wendland et al., 2007). For example, according to Molle et al (2018), the aquifer of the delta of Nile river is semi-confined, as its top is covered by a thin clay layer whose thickness varies from 5 m in the south to 20 m in the middle and 50 m in the north of the Delta, while disappearing in some places (Mabrouk et al., 2013). The infiltration values are associated with a total recharge rate of 6.78 Bm³/y (FAO 2013). However, this key term of the water balance is extremely difficult to measure or estimate and is not known with much accuracy. Groundwater modeling studies generally neglect the contribution of rainfall with an average between 25 and 200 mm/year to recharge since it is very small compared to the recharge rate (Mabrouk et al., 2013). It is therefore not considered. Groundwater in the Delta is not a separate or additional resource and is directly fed by surface water brought by the Nile River.

Physico-Chemical Parameters

The origin of the physico-chemical composition of the water of the San Diego aquifer depends on the geological formation; requiring a hydrogeochemical analysis. The San Diego aquifer is included in the igneous-metamorphic units belonging to the “Cordillera de La Costa”, being constituted by a metamorphic association where gneiss and marble predominate (Urbani, 2016). The San Diego aquifer is divided by rocks of two geological periods, which are: 1) triassic covering the north and central region and

2) quaternary in the south region around the Valencia Lake (Hackley et al., 2005). The gneiss is a metamorphic rock composed of the minerals such as quartz, feldspar and mica. Marble is a metamorphic rock composed of recrystallized carbonate minerals, most commonly calcite or dolomite. The water of San Diego aquifer has been classified by the diagram of Piper-Hill-Langelier (Piper, 1944), in four classes (Figure 17): 1) Bicarbonate of Calcium and/or Magnesium Ca-Mg-HCO₃ (North and Central regions, 95.16 km², 81.25%) 2) Bicarbonate of Sodium Na-HCO₃ (Central and South regions, 19.32 km², 16.5%), 3) Sulfate or Chloride of Calcium and/or Magnesium Ca-Mg-SO₄ and Ca-Mg-Cl (South region, 0.96 km², 0.82%), 4) Sulfate and/or Chloride of Sodium Na-SO₄ and Na-Cl (South region, 1.68 km², 1.43%). The division between the main water compositions corresponding to the water classes 1 and 2-4 of the San Diego aquifer is coincident with the division of rocky material according to the geological periods. The conditions under which the interactions between solid and liquid phases occur depend on mainly of the weathering of rock-forming minerals. For the weathering of rock-forming minerals, the solution kinetics is determined by the solubility product and transport in the vicinity of the solid water-interface. If the dissolution rate of a mineral is higher than the diffusive transport from the solid-water interface, saturation of the boundary layer and an exponential decrease with increasing distance from the boundary layer results (Merkel and Planer-Friedrich, 2005). The reaction rate mainly depends on the concentration of reactants and products, pH, light, temperature, organics, presence of catalysts, and surface-active trace substances can have a significant influence on reaction rates. In the case of San Diego aquifer, the conditions to carry out the reaction rate are (Figure 12): pH between 6 and 8, Temperature between 27

and 28 °C, Electrical conductivity between 188 and 2341 μ S/cm. The pH and temperature have an insignificant variation, while the electrical conductivity changes significantly between the north and central regions with respect to the south region, founding a low mineralization in the north and central regions (188 < CE < 2341 μ S/cm) where there is a boundary between the classes 1 and 2, likewise in the south region, the water is highly mineralized and its composition corresponds to the classes 2-4 (Figure 12). By comparing with other studies, Martos-Rosillo and Moral (2015) have found that the water of Becerro aquifer, Spain, is fundamentally HCO₃Ca. In some particular points, the water may become HCO₃Cl-CaNa, points in which there is a near contact between Jurassic and Triassic materials; being relatively low in mineralization (269 < CE < 813 μ S/cm), while the waters with sodium chloride are highly 256 mineralized (2280 < CE < 9196 μ S/cm); being a pattern observed in both aquifers.

Hydraulic Parameters

The water dynamic level in the San Diego aquifer shows the minimum values to the central region of the aquifer (Figure 13). The zone, where the minimum water level occurs is rounded by the maximum water level in the aquifer during the period 2015-2017. This is a residential zone, being the water use of domestic type. The maximum hydraulic gradient is estimated that occurs in the central and mountains regions (Figure 14). The maximum hydraulic gradient combined with the minimum water dynamic level allows to detect a potential zone where a water overexploitation of aquifer might be occurring. Likewise, it might be due to the lack of maintenance of the grids belonging to the perforated pipe that protects the walls of the well, causing the water that supplies to the well has a small discharge, increasing the depth where the piezometric

head can be found and justifying the maximum hydraulic gradient. In the mountains zone, the hydraulic gradient is maximum because of the natural relief. The flow velocities estimated of San Diego aquifer vary between 1259 and 2023 m/d; being close to those measured in the aquifer system in the transboundary area of the Soča/Isonzo river basin (Slovenia/Italy) reaching values between 1344 and 2280 m/d, which vary between 1344 and 2880 m/d (Vižintin et al., 2018).

Mass flow of physico-chemical parameters

Mass flow of physico-chemical parameters give as a result that, in general, the maximum mass flow occurs in the highest terrain elevation zones of San Diego aquifer and there is a slight trend to occur in the south region in the proximity to the Valencia Lake (Figure 16). In the north region, the mass flow is influenced by terrain gradient and the soil type, increasing the dissolution rate of a mineral is and the diffusive transport from the solid-water interface. In the south region, it might be occurring an inverse hydraulic gradient from Valencia Lake to San Diego aquifer during the dry season, incorporating the water of the Valencia Lake to the San Diego aquifer and increasing the concentration of the physico-chemical parameters in the south region of the San Diego aquifer (Figure 16). Gorai and Kumar (2006) have applied models of spatial distribution of groundwater quality parameters such as Ca, Mg, pH, Mn, Fe, Nitrate, Turbidity, Na, K, TDS, Alkalinity Total Hardness concentrations were carried out through GIS and Geostatistical techniques, founding that deterioration of ground water quality is not very serious problem except few areas.

CONCLUSIONS

-The San Diego aquifer includes alternating layers of soil material predominantly between well-graded sand and clay of low plasticity, being confined aquifer. The gravel is the unique aquifer material in the three profiles close to the mountain zone identified as: PW5, PW19 and PW27 where the recharge zones might be located.

-The San Diego aquifer is a source of water and storage reservoir; being a renewable resource because of the precipitation; which depends on the distribution of storms, land topography and cover, permeability of soil, infiltrates through the ground surface and replenishes the underlying phreatic aquifer. Hydrological processes in the San Diego aquifer such as infiltration and permeability are influenced by the impermeability in the urban area of the San Diego aquifer, which is around 20% of the total area, reducing the contribution rates to the aquifer water.

- The volume stored in the San Diego aquifer is giving negative results based on this is estimated only by three variables: 1) infiltration, which is the unique water inlet, 2) evapotranspiration and 3) pumping flow; which are water outlet. It must be considered other sources of direct recharge from the San Diego River.

-The division between the main water compositions corresponding to the water classes 1 and 2-4 of the San Diego aquifer is coincident with the division of rocky material according to the geological periods Triassic and quaternary, respectively, being the water classes: 1) Bicarbonate of Calcium and/or Magnesium Ca-Mg-HCO_3 (North and Central regions, 95.16 km^2 , 81.25%) 2) Bicarbonate of Sodium Na-HCO_3 (Central and South regions, 19.32 km^2 , 16.5%), 3) Sulfate or Chloride of Calcium and/or Magnesium Ca-Mg-SO_4 and Ca-Mg-Cl (South region, 0.96 km^2 , 0.82%), 4) Sulfate and/or Chloride of Sodium Na-SO_4

and Na-Cl (South region, 1.68 km^2 , 1.43%).

-With respect the quality of water in the San Diego aquifer, the pH and temperature have an insignificant variation, while the electrical conductivity changes significantly between the north and central regions with respect to the south region, founding a low mineralization in the north and central regions ($188 < \text{CE} < 2341 \mu\text{S/cm}$) where there is a boundary between the classes 1 and 2, likewise in the south region, the water is highly mineralized and its composition corresponds to the classes 2-4.

-The maximum hydraulic gradient is estimated that occurs in the central and mountains regions. The maximum hydraulic gradient combined with the minimum water dynamic level allows to detect to the central zone as a potential zone where a water overexploitation of aquifer might be occurring.

- In the north region, the mass flow is influenced by terrain gradient and the soil type, increasing the dissolution rate of a mineral is and the diffusive transport from the solid-water interface. In the south region, it might be occurring an inverse hydraulic gradient from Valencia Lake to San Diego aquifer during the dry season, incorporating the water of the Valencia Lake to the San Diego aquifer and increasing the concentration of the physico-chemical parameters in the south region of the San Diego aquifer.

- The modeling of the hydrogeochemical parameters is represented by J-Bessel function.

REFERENCES

1. Box, G. E. P., Jenkins, G. M., and Reinsel G. C. (1994). Time Series Analysis: Forecasting and Control. 3rd ed. Englewood Cliffs, NJ: Prentice Hall, 1994.
2. FAO, 2013. Monitoring of Climate Change Risk Impacts of Sea Level

- Rise on Groundwater and Agriculture in the Nile Delta. TCP/EGY/3301.
3. Gandin, L.S., 1960. On optimal interpolation and extrapolation of meteorological fields. *Trudy MainGeophys. Obs.* 114, 75–89.
 4. Guevara Pérez, E. (2000). Diagnóstico de la situación ambiental y ecológica del Estado Carabobo. *Revista Ingeniería UC*, 7(1).
 5. Guevara, E., & Cartaya, H. (2004). *Hidrología ambiental*. Facultad de Ingeniería de la Universidad de Carabobo. Valencia, Venezuela.
 6. Gorai, A. K., & Kumar, S. (2013). Spatial distribution analysis of groundwater quality index using GIS: a case study of Ranchi Municipal Corporation (RMC) area. *GeoinformGeostatOverv*, 1, 2.
 7. Hackley, P. C., Urbani, F., Karlsen, A. W., & Garrity, C. P. (2005). Geologic shaded relief map of Venezuela (No. 2005-1038).
 8. Hengl, T. (2009). A practical guide to geostatistical mapping (Vol. 52). Hengl.
 9. INE (2001). Censo 2001. Instituto Nacional de Estadísticas. Available: http://www.ine.gov.ve/index.php?option=com_content&view=category&id=95&Itemid=9. Date: 08-11-2018.
 10. INE (2011). Censo. Instituto Nacional de Estadísticas. Available: http://www.ine.gov.ve/index.php?option=com_content&view=category&id=95&Itemid=9. Date: 08-11-2018.
 11. IESA (1998) Carabobo: Competitividad para el desarrollo volumen XI.
 12. Kranjc, A. (Ed.), 1997. Karst hydrogeological investigations in South-Western Slovenia. *Acta Carsologica* 26 (1) (388 pp).
 13. Krige, D. G. (1951). A statistical approach to some basic mine valuation problems on the Witwatersrand. *Journal of the Southern African Institute of Mining and Metallurgy*, 52(6), 119-139.
 14. Mabrouk, M.B., Jonoski, A., Solomatine, D., Uhlenbrook, S., 2013. A review of seawater intrusion in the Nile Delta groundwater system –the basis for assessing impacts due to climate changes and water resources development. *Hydrol. Earth Syst. Sci.* 10, 10873–10911, Discussions.
 15. Marotz, G. (1968). *TechnischeGrundlageneinerWasserspeicherungimnatürlichenUntergrund*. Eigenverl. d. Instituts f. Wasserwirtschaft, Grundbau u. Wasserbau d. Universität Stuttgart.
 16. Marquez A., Guevara E., Rey D. (2018). Assessment of Land Use and Land Cover Change Detection Using Eleven Techniques of Satellite Remote Sensing in the Pao River Basin, Venezuela. *Journal of Remote Sensing GIS and Technology*, 4 (2), 1-70.
 17. Martos-Rosillo, S., & Moral, F. (2015). Hydrochemical changes due to intensive use of groundwater in the carbonate aquifers of Sierra de Estepa (Seville, Southern Spain). *Journal of Hydrology*, 528, 249-263.
 18. Matheron, G. (1963). Principles of geostatistics. *Economic Geology*, 58, 1246–1266.
 19. Matthes, G., & Ubell, C. (2003). *AllgemeineHydrogeologie, Grundwasserhaushalt–Lehrbuch der Hydrogeologie Bd. 1*. GebrüderBorntraeger, Berlin, Stuttgart.
 20. Molle, F., Gaafar, I., El-Agha, D. E., & Rap, E. (2018). The Nile delta's water and salt balances and implications for management. *Agricultural Water Management*, 197, 110-121.
 21. Morsy, W.S., (2009). *Environmental Management to Groundwater Resources for NileDelta Region*, PhD Thesis. Faculty of Engineering, Cairo University, Egypt.
 22. Pérez, E. G., & Romance, A. M. (2012). Modelación de la infiltración

- en un campo agrícola de la cuenca del río Chirgua, estado Carabobo, Venezuela. *Revista Científica UDO Agrícola*, 12(2), 365-388.
23. Piper, A.M., (1944). A graphic procedure in the geochemical interpretation of water-analyses. American Geophysical Union. *Papers, Hydrology*, pp. 914-923.
 24. Ramirez, L. E. (1971). Development of a Procedure for Determining Spatial and Time Variations of Precipitation in Venezuela.
 25. Trezza, R. (2006). Evapotranspiration from a Remote Sensing Model for Water Management in an irrigation system in Venezuela. *Interciencia*, 31(6).
 26. Urbani, F. (2016). Synthesis of the nomenclature of the igneous and metamorphic rocks units of the cordillera de la costa, venezuela. *Revista de la Facultad de Ingeniería*, 31(2).
 27. Vižintin, G., Ravbar, N., Janež, J., Koren, E., Janež, N., Zini, L., ...& Petrič, M. (2018). Integration of models of various types of aquifers for water quality management in the trans boundary area of the Soča/Isonzo river basin (Slovenia/Italy). *Science of The Total Environment*, 619, 1214-1225.
 28. Wendland, E., Barreto, C. E. A. G., & Gomes, L. H. (2007). Water balance in the Guarani Aquifer outcrop zone based on hydrogeological monitoring. *Journal of Hydrology*, 342(3-4), 261-269.
 29. Zeidan, B.A., 2016. Groundwater Monitoring, Modeling and Assessment in the NileDelta (Unpublished chapter).